中央大学博士論文

Synthesis and Property of Diboryldiphosphene

Asami Shunsuke
浅見　俊介

博士（工学）

中央大学大学院
理工学研究科
応用化学専攻

平成２８年度
２０１７年3月

Chapter 1, General Introduction

Chapter 2, A Boryl-Substituted Diphosphene: Synthesis, Structure, and Reactivity with ^{n}BuLi to Form An Isolable Adduct Stabilized by pπ-pπ Interactions

Abbreviations: The following abbreviations have been used where relevant

Å	angstrom
B3LYP	Becke, three-parameter, Lee-Yang-Pair
Bbt	2,6-bis[bis(trimethylsilyl)methyl]-4-[tris(trimethylsilyl)methyl]phenyl
Bcat	benzo[1,2-*c*]-1,3,2-dioxaborolan-2-yl
Bu	butly
Bpin	4,4,5,5-tetramethyl-1,3,2-dioxaborolan-2-yl
Bz	benzoyl
CAAC	cyclic(alkyl)(amino)carbenes
CAM	Coulomb-attenuating method
Cp	cyclopenta-2,4-dien-1-yl
cryptand	1,10-diaza-4,7,13,16,21,24-hexaoxabicyclo[8.8.8]hexacosane
Cy	cyclohexyl
D	deuterium
d	doublet
δ	chemical shift
DFT	density function theory
Dip	2,6-diisopropylphenyl
DMAP	*N*,*N*-dimethyl-4-aminopyridine

DME	1,2-dimethoxyethane
DPFGSE-TOCSY	double pulse field gradient spin echo totally correlated spectroscopy
ESR	electron spin resonance
Et	ethyl
FAB	fast atom bombardment
fwhm	half width at half maximum
GOF	goodness of fit
HOMO	highest occupied molecular orbital
HRMS	high-resolution mass spectrometry
LUMO	lowest unoccupied molecular orbital
m	multiplet
Me	methyl
Mes	2,4,6-trimethylphenyl
Mes*	2,4,6-tri-*tert*-butylphenyl
n	normal
NBO	natrural bond orbital
NHC	N-heterocyclic carbene
Np	neopentyl
NMR	nuclear magnetic resonacne
ORTEP	Oak Ridge thermal ellipsoid plot

Ph	phenyl
Pr	propyl
q	quartet
s	singlet
sep	septet
SOMO	singly occupied molecular orbital
t	triplet
Tbt	2,4,6-tris[bis(trimethylsilyl)methyl]phenyl
TD-DFT	time-dependent DFT
THF	tetrahydrofuran
TMS	trimethylsilyl
Tmp	2,2,6,6-tetramethylpiperidinyl
Trip	2,4,6-triisopropylphenyl
UHF	unrestricted Hartree-Fock
WBI	Wiberg bond index

Chapter 1

General Introduction

1.1, The first isolation of diphosphene

Main group elements of the later third period are defined as heavier main group elements. However, its double bond species had not been isolated until recently due to oligomerization through intermolecular P-P bond formation and hydrolysis under ordinary conditions. Because of longer element-element bond between the third or higher period elements than those of second low elements, overlap of two p-orbitals is reduced to form π-bond. In addition, Power estimated bond cleavage energy about π–bonding of double bond species.[1] These results have shown heavier double bond species have weaker π–bonding than double bond species of second low elements (Table 1). Although K ü hler and Michael reported the synthesis of "Ph-P=P-Ph" by the condensation reaction between $PhPCl_2$ and $PhPH_2$ in 1877, structure was later turned out to be wrong (Scheme 1.1).[2] Later, Daly confirmed by X-ray structure analysis that it was the mixture consisted of pentaphenylcyclopentaphosphane and hexaphenylcyclohexaphosphane.[3]

Table 1. Relative energies (kcal/mol) of σ and π bonds in homo nuclear main group diatomic species

B-B	70	C-C	81/**62**	N-N	38/**94**
Al-Al	36	Si-Si	42/**28**	P-P	48/**34**
Ga-Ga	32	Ge-Ge	39/**26**	As-As	35/**28**
In-In	23	Sn-Sn	35/**11**	Sb-Sb	31/**20**
Tl-Tl	2	Pb-Pb	23	Bi-Bi	21/**10**

Thin font ••• σ bond
Bold font ••• π bond

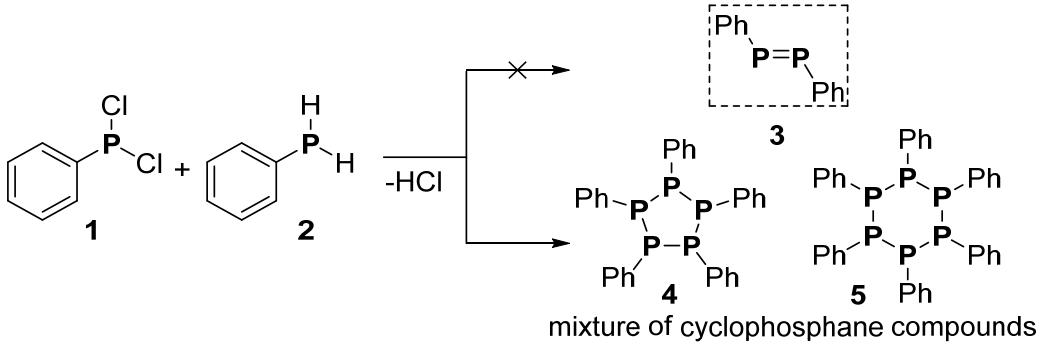

Scheme 1.1 Reports of condensation between $PhPCl_2$ and $PhPH_2$

While, kinetic stabilization by using very bulky substituents enables to provide an efficient construction of stable heavier double bond species. West *et al.* synthesized the first stable disilene via the dimerization of the corresponding 2,4,6-trimethylphenyl(Mes)-substituted silylene generated by the photolysis of a trisilane (Scheme 1.2).[4]

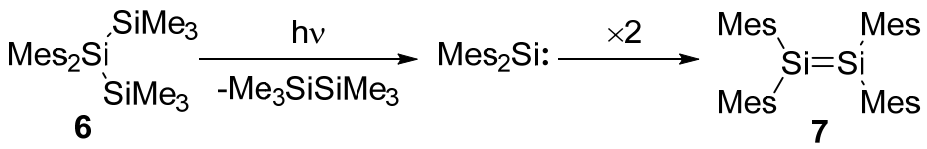

Scheme 1.2 Synthesis of the first stable disilene

For example, the first stable diphosphene as bis(2,4,6-tri-tert-butylphenyl)diphosphene (Mes*-P=P-Mes*) was reported by Yoshifuji in 1981(Scheme 1.3). [5] The reduction of Mes^*PCl_2 with magnesium in THF led to the formation of orange-red crystalline solids as a thermally stable compound. Since this reports, the basic properties of the first synthesis kinetically stabilized diphosphene have been clarified.

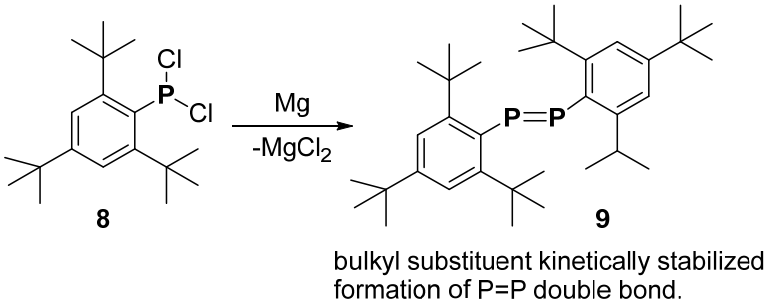

Scheme 1.3 Synthesis of the first stable diphosphene

1.2 Structural, optical, and electrochemical property of diphosphene

Diphosphene has characteristic structure in comparison with that of azo-compound. For example, P-P-C angle of Mes*P=PMes* is smaller than that of N-N-C angle of Ph-N=N-Ph (P-P-C = 102.8 (1), vs N-N-C 121.5(3)). [6] This difference is due to inert pair effect derived from heavier element.[7] The outermost atomic s orbital in heavier element have a tendency not to participate bond formation. The 3p and 3s orbital of a phosphorus atom have low tendency to form sp^2 hybrid orbitals. Therefore, σ and π bonds with high p character have been formed in diphosphene (Figure 1.1).

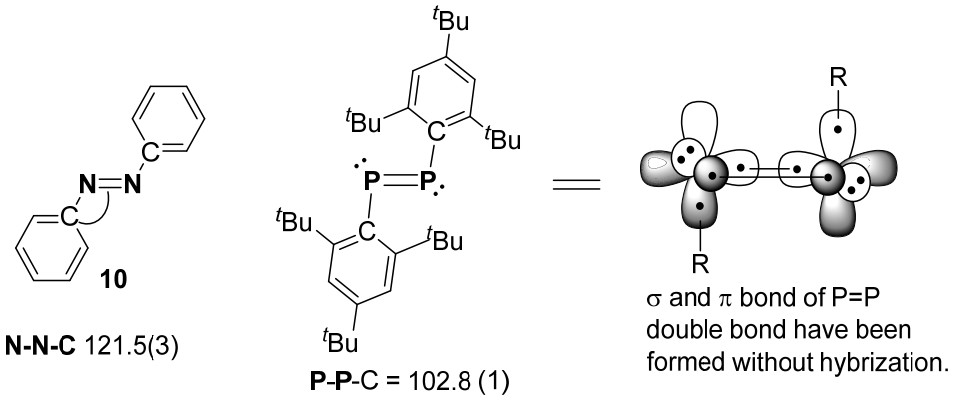

Figure 1.1. Structure difference between diphosphene and azobenzene

While the absorption spectra of diphosphenes exhibited two maxima in the range of 300 to 500 nm.[8] These absorptions are ascribed to the n-π* and π–π* transitions derived from the P=P double bond moiety of diphosphene. However, the absorption in the longer-wavelength caused by n→π* transition is considerably less intense than the shorter-wavelength of π→π*. Because the former transition is symmetry forbidden against the latter of symmetry allowed transition. While diphosphene species are known to be more easily reduced than azo-compounds.[9] Cyclic voltammetry of Mes*P=PMes* in acetonitrile using $(^nBu_4N)BF_4$ as an electrolyte and a Pt electrode exhibited a reversible reduction at -1.93 eV vs. SCE in THF.[10] In addition, ESR studies for

diphosphene radical anions, which were generated by one-electron reduction, have been reported (Figure 1.2). The triplet signal in the ESR spectrum of the diphosphene anion radical can be assigned to interaction between the unpaired electron and two magnetically equivalent ^{31}P nuclei [g = 2.007 – 2.018: a(^{31}P) = (43-55 G):(g: *Landé* g-factor, a: hyperfine coupling constant)], which are consistent with the singly occupied π^* orbital of P=P moiety.[11]

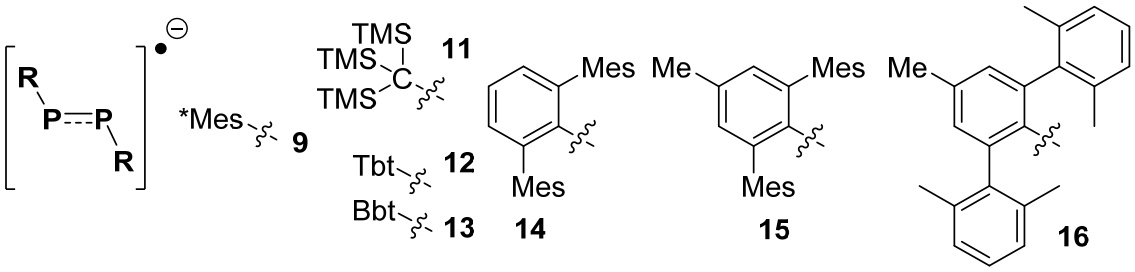

Figure 1.2. Examples of diphosphene radical anions detected by ESR (TMS = $SiMe_3$, Mes = 2,4,6-$Me_3C_6H_2$, Mes* = 2,4,6-^{t}Bu$_3$C$_6$H$_2$, Tbt = 2,4,6-[$(Me_3Si)_2CH]_3C_6H_2$, Bbt = 2,6-[$(Me_3Si)_2CH]_2$-4-[$(Me_3Si)_3C]C_6H_2$)

1.3 Substituent effect toward the property of diphosphene

Substituents have a greater influence on the property of diphophene. Mes*P=P-N(^{i}Pr)$_2$ **17** and Mes*P=P-TMP **18** (TMP = 2,2,6,6-tetramethylpiperidinyl), where the lone pair of the nitrogen atoms conjugated with the P=P double bond.[12] **17** and **18** have shorter P-N bond length than that of diamino-substituted diphosphene **19**. Because the structure of **19** has a perpendicularly relation between nitrogen substituents and the π-bonding of P=P.[13] Moreover, N-P-P bond angles of **17** and **18** were wider than those of C-P-P bond angles. Therefore, one of resonance structures of **17** and **18** could be described as X', which has P=N double bond and negative charge on phosphorus at β position.

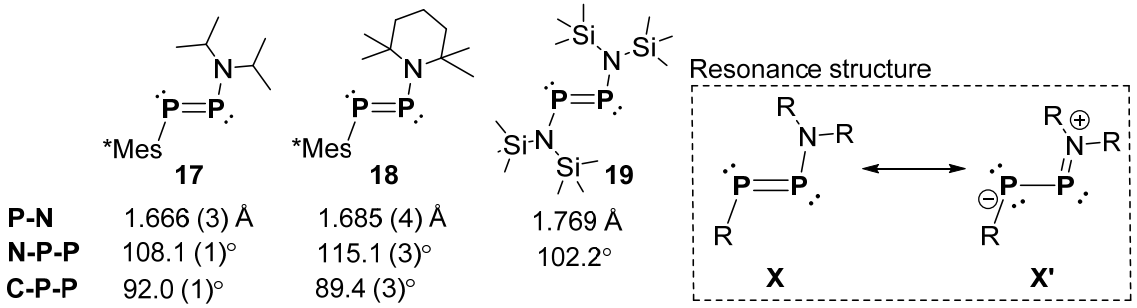

Figure 1.3. Influence of amino substituent on the structure of diphosphenes

Ferrocenyl-diphosphene **20** has a unique optical property,[14] that is, it exhibited red-shifted absorption at λ_{max} 542 nm toward λ_{max} 460 nm of Mes*P=PMes*, because of d–π* electron transitions from d-orbitals at the Fe center to the π* orbital of the P=P double bond (Figure 1.4). Although these reports have shown importance of substituent effect, the introduction of 13 elements into diphosphene has not been reported.

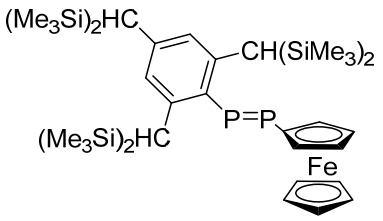

20

Ferrocenyl-substituted diphosphene has red-shifted absorption (λ_{max} 542 nm) toward that of Mes*-diphosphene (λ_{max} 460 nm).

Figure 1.4. Ferrocenyl-substituted diphosphene **20**

1.4 Reaction of diphosphene with alkyllithium.

Yoshifuji and Cowley reported the nucleophilic addition of alkyllithium to Mes*P=PMes* **9** and the subsequent quenching of the obtained Mes*(R)P-PMes*(Li) [R = ^{n}Bu (**21**), Me (**24**)] by proton source or a variety of alkyl halides.[15,16] Yoshifuji reported the synthesis of the corresponding diphosphene monosulfide **22** via **21** as intermediate, which was only detected by ^{31}P NMR spectroscopy (Scheme 1.4). The intermediate of **24** has been converted to diphosphine by reaction with methanol. However, it was described that isolation of **24** was difficult due to its high reactivity (Scheme 1.5). Ito has reported the unprecedented reactivity of **21** with various benzoyl chloride giving phosphaalkene **23** through a cleavage of P-P bond.[17]

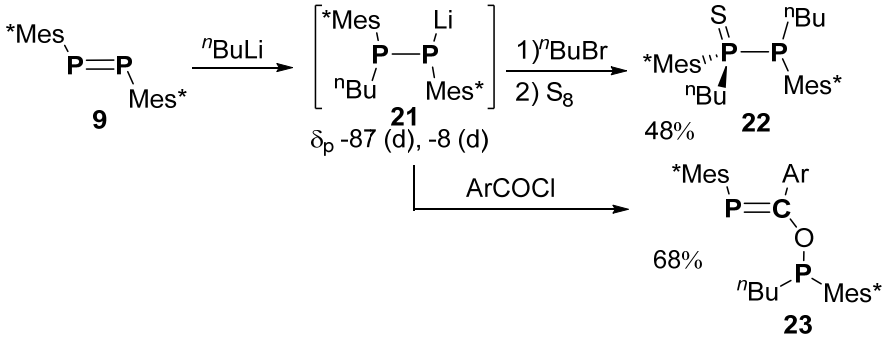

Scheme 1.4. Reaction of ^{n}BuLi-Mes*P=PMes* adduct

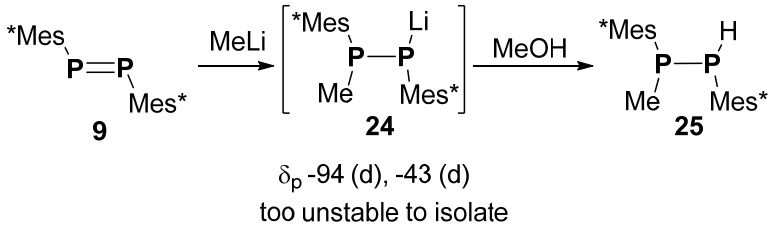

Scheme 1.5. Reaction of MeLi-Mes*P=PMes* adduct

1.5 σ–donor ability of boryl-substituent

Boron has electropositive character in comparison with that of carbon atom (Pauling electronegativity: Boron: **2.20** Carbon **2.55**). The palladium complex **26** has shown strong σ donor property of boryl ligand. The bond length of P-Pd in **26**, which is trans-position of boryl ligand, is longer than bond lengths of P-Pd of trans-position for stannyl or alkyl ligand in **26** and **27** (Figure 1.5). These results have shown that boryl ligand has stronger σ

donor property than those of alkyl- and stannyl-ligand.[18] Moreover, σ-donor property of boryl-ligand has been comparable to silyl ligand, which is known as one of the strongest σ donor ligands. The bond length of P-Pd of trans-position for silyl-ligand in **28** is similar to that of P-Pd of trans-position for boryl-ligand in **26**. In addition, . Marder has investigated strength of σ-donor property of boryl ligand by computational analysis. In square planar platinum complex, boryl ligand showed stronger trans-influence in comparison with those of anionic group 14 element ligands.[19]

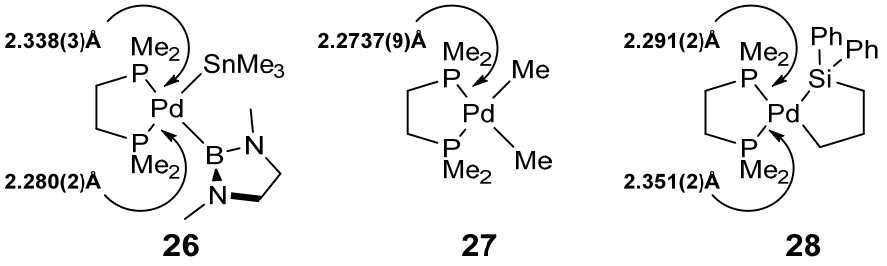

Figure 1.5. Trans influence of boryl ligand in Pd complex

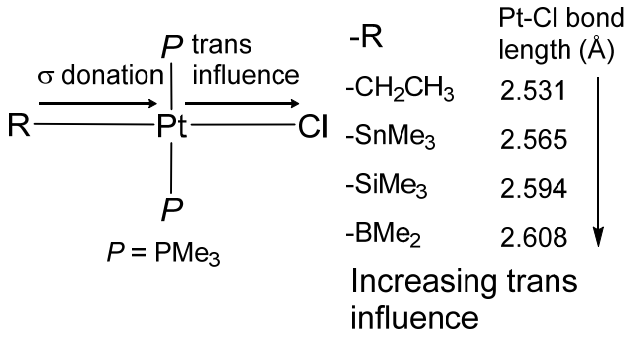

Figure 1.6. Trans influence of boryl ligand in Pt complex

1.6 The π acceptor property of boryl substituent and pπ–pπ interaction in phosphorus and boron – containing compounds

Boryl substituent is known to interact with an adjacent heteroatom through pπ–pπ interaction. For example, aminoborane has short B-N bond distance 1.38 Å (av.) in comparison with that of an amine-borane (1.58 Å (av.)), the planar core geometry, and the high activation barrier of B-N bond rotation (Figure 1.7).[20]

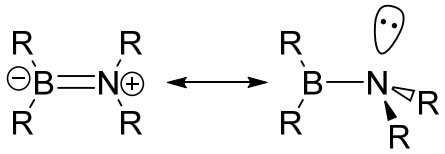

Figure 1.7. pπ-pπ interaction of aminoborane

While a phosphino-borane have a strong tendency to associate and they are given as oligomeric rings having B-P frameworks with four-coordinate B and P centers. Bung has reported trimer and tetramer of $(CH_3)_2PBH_2$,[21]

Further Goldstein detected the structure of tetramer species by X-ray analysis.[22] However, recently, Power has reported some monomeric phosphino-borane and boryl-phosphide have shorter P-B bond lengths than that of phosphine-borane (Figure 1.8), because of pπ–pπ interaction between boron and phosphorus atom.[23]

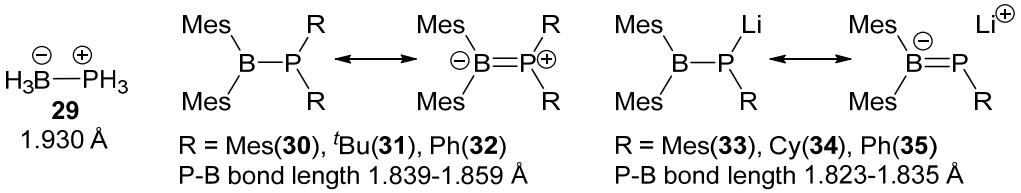

Figure 1.8. pπ-pπ interaction of phosphino-borane and boryl-phosphide

1.7 Nucleophic borylation of boryllithium

Segawa, Nozaki, and Yamashita reported synthesis of boryl anion by a reduction of bromoborane possessing a five-membered ring and bulky Dip group with lithium naphthalenide and its characterization (Scheme 1.5).[24] In addition, the boryllithium **37** reacted with various organic electrophile such as alkyl halides, carbonyl compounds, proton source and fluoroarenes to form addition or nucleophilic substitution products (Scheme 1.6). Furthermore, boryl-substituted main group element compounds and metal-complexes can be synthesized by the reaction of boryllithium via nucleophilic borylation (Scheme 1.7(a)).[24n] The author expected this diaminoboryl-substituent would have a strong σ-donor ability by low electronegativity of boron atom and would accept π-electron from adjacent atom, although nitrogen atoms donate electron to boron atom (Scheme 1.7(b)).

.

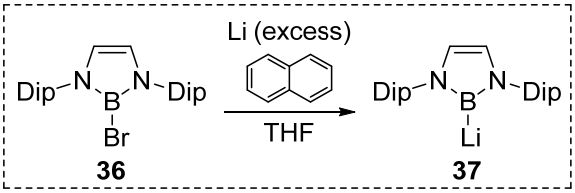

Scheme 1.5. Synthesis of boryllithium (Dip = 2,6-$^{i}Pr_2C_6H_3$)

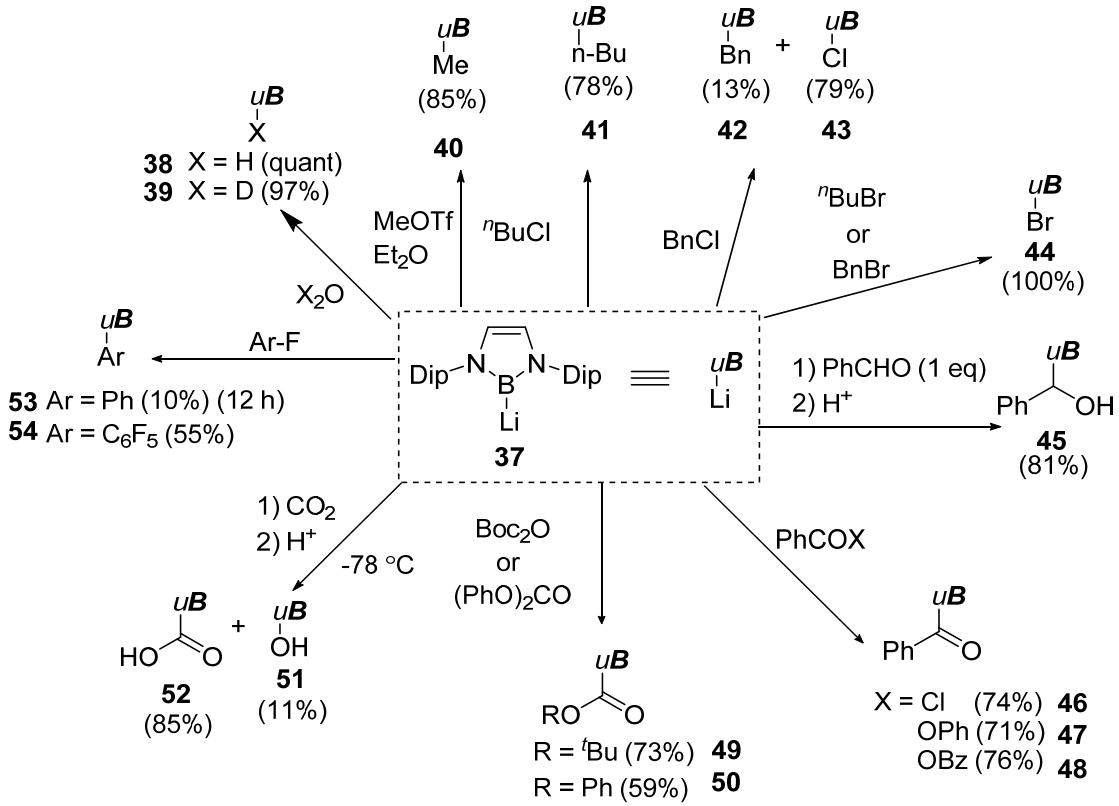

Scheme 1.6. Reaction for boryllithium with electrophiles

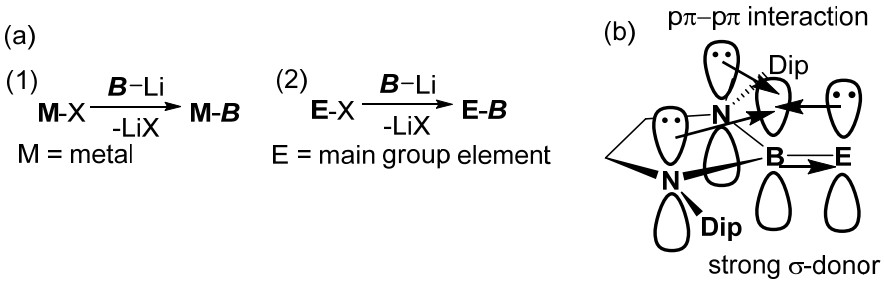

Scheme 1.7. (a) Synthetic methods for boryl-substituted transition metal complexes and main-group-element compounds (b) effect of diaminoboryl substituent

1.8 Low-coordinated main group compounds possessing boryl substituents

Boryllithium has been utilized for the synthesis of boryl-substituted main group compounds. Aldridge *et. al.* have reported boryl-substituted silylene **55**, germylene **56**, and stannylene **57** via nucleophilic borylation.[25] Among them, boryl-substituted acyclic silylene has reacted with hydrogen gas, and it has been transformed into corresponding hydrosilane **58** (Scheme 1.8). From the DFT calculations of this reaction, it was revealed σ-bond of H_2 molecule coordinates to vacant p-orbital of silylene in transition state. In addition, diborylstannylene **59** and diboryllead **60** could be synthesized by the reaction of $SnCl_2$ or $PbBr_2$ with boryllithium.[26]

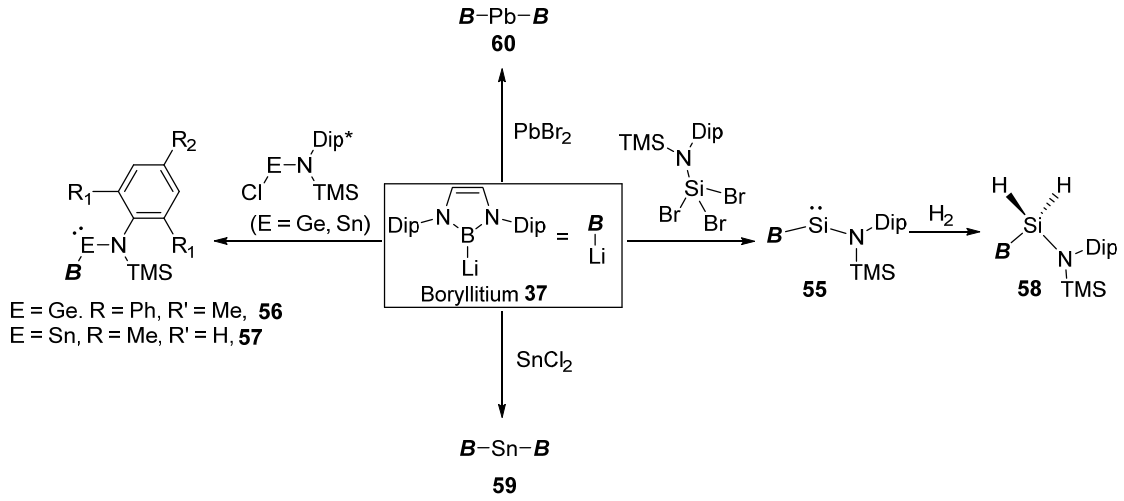

Scheme 1.8. Synthesis of boryl-substituted divalent group 14 element compound

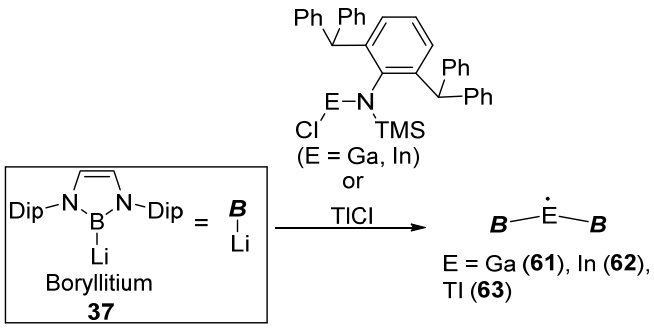

Scheme 1.9. Synthesis of boryl-substituted divalent group 13 element compound

They also reported the first thermally stable monomeric divalent radicals of gallium, indium, and thallium.[27] X-ray structures of these compound revealed a bent B-M-B structure (M = Ga **61**, In **62**, Tl, **63**) and all of three radicals were characterized to have spin density mainly at the metal center by ESR spectra and DFT calculations. The authors stated that bulky boryl substituent affected reactivity and stability of these low coordinated species.

1.9 Synthesis of boryl-substituted group 15 element compound via nucleophilic borylation

As the first example of nucleophilic borylaton of group 15 elements, Gudat reported the reaction of boryllithium with diaminochlorophosphines to give the corresponding borylphosphines **64** and **65**.[28]

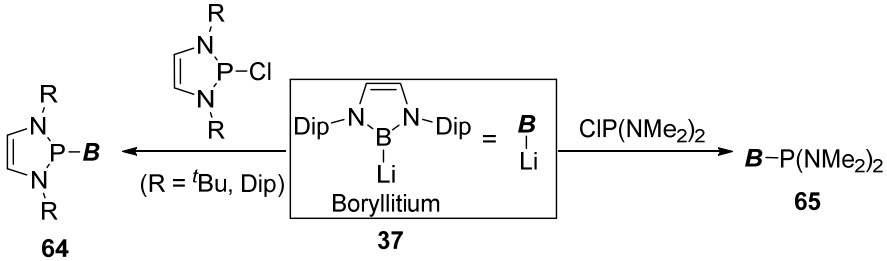

Scheme 1.10. Synthesis of boryl-substituted phosphorus compounds

However, pπ–pπ interaction of B and P in these compounds was concluded to be significantly small. Because the P-B bond length of **64** [B-P 1.951(2) Å] was longer than those of previous phosphino-boranes [B-P bond length: 1.839-1.859 Å]. In addition, NBO analysis of model compound **64'** indicated that the lone pair of N atom largely interacted with the vacant p orbital of boron in contrast to the small interaction between B and P.

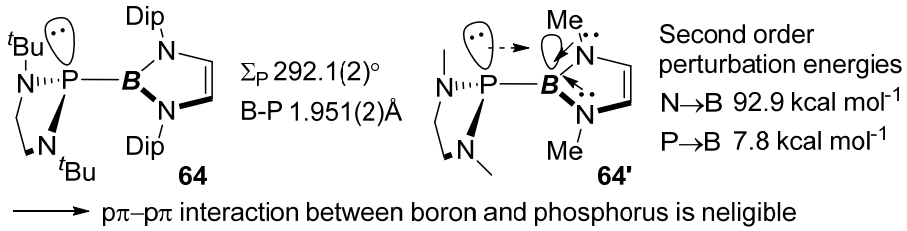

Figure 1.11. Property of diaminophosphino-borane

Recently, Kinjo reported boryllithium **65** possessing a triazaborole skeleton, which underwent transmetallation to magnesium and subsequently reacted with 1 equiv of Ph_2SbCl and Ph_2BiCl[29] to afford boryl-substituted diphenylstibane **67** and diphenylbismuthane **68**, respectively (Scheme 1.8). However, these reports they did not deal with dihalogeno-substituted pnictogen species, which have been known as precursors of doubly bonded compounds between group 15 elements.

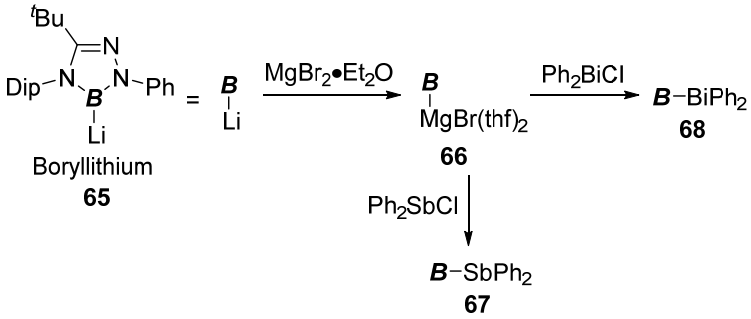

Scheme 1.12. Synthesis methods for boryl-substituted antimony and bismuth compounds

1.10 Boryl-substituted heavier double bond species

Previously, There are few reports of Boryl-substituted heavier double bond species. Sekiguchi synthesized the boryl-substituted disilenes (^{t}Bu$_2$MeSi)$_2$Si=Si(SiMe^{t}Bu$_2$)(BR*$_2$) (R* = pinacol **69**, catechol **70**) by the reaction of disilenyllithium (^{t}Bu$_2$MeSi)$_2$Si=Si(SiMe^{t}Bu$_2$)Li **71** with (pin)BCl or (cat)BCl.[30] In addition, they also have shown to prepare **72** and **73** via hydroboration of disilyne **74** with 9-BBN or (cat)BH.[31] Moreover, **72** have smaller torsion angle between boryl moiety and Si=Si moiety (Si-Si-B-C = 18º) than that of **73** (Si-Si-B-O = 52º). Therefore, the absorption maxima of **72** (λ_{max} = 469 nm), was redshift in comparison with that of **73** (λ_{max} = 411 nm). This result can be considered to be ascribable to extension of π-conjugation of **72** by vacant p-orbital at boron.

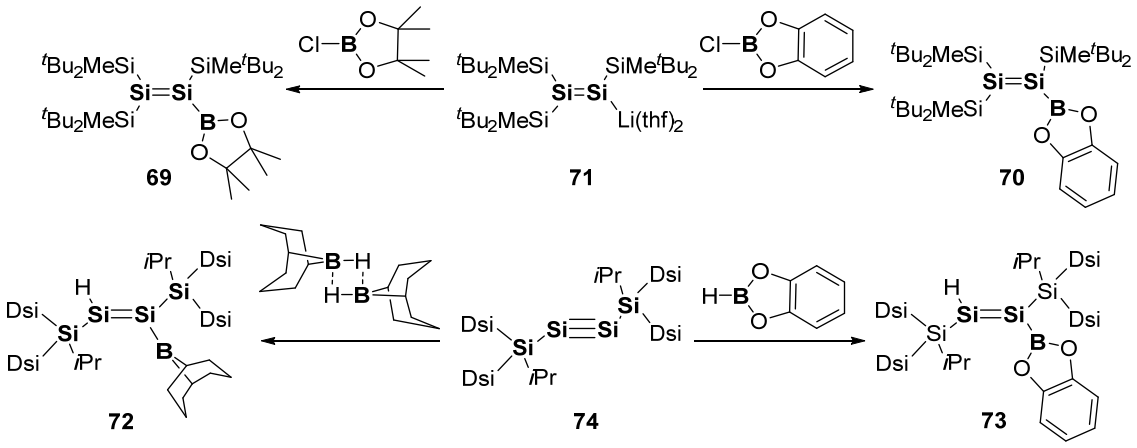

Scheme 1.13. Synthetic methods of boryl-substituted disilene

While Aldridge reported the synthesis of boryl-substituted digermyne-NHC (N-heterocyclic carbene)[32] adduct **76** through reduction of NHC-stabilized (boryl)germanium chloride **75** with Jones' reagent.[33]

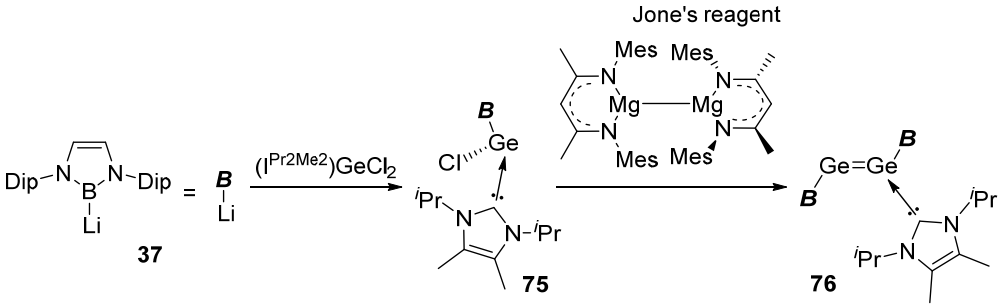

Scheme 1.14. Synthesis of boryl-substituted digermyne

Diboryl-dibismuthene is the sole isolated example of boryl-substituted heavier double bond species consisting of group 15 element, which was synthesized by the reaction of boryllithium and (amino)(dibromo)bismuthane **77**.[34] Aldridge has proposed that **80** would be generated by the reaction intermediate, diamino-dibismuthene **79** with boryllithium(Scheme 1.15). The structure of **80** was confirmed as co-crystal consisting of $\mathbf{80}_{plan}$ and $\mathbf{80}_{orth}$ by X-ray analysis. Although $\mathbf{80}_{plan}$ has coplanar relation between boryl-substituent and B_2Bi_2 plane, $\mathbf{80}_{orth}$ has orthogonal relation between boryl-substituent and B_2Bi_2 plane (Figure 1.12). The B-Bi bond lengths in the both structures are 2.326(7) Å ($\mathbf{80}_{plan}$) and 2.317(9) Å ($\mathbf{80}_{orth}$), respectively, and these values are close to the sum of the covalent radii for B and Bi (2.32 Å).

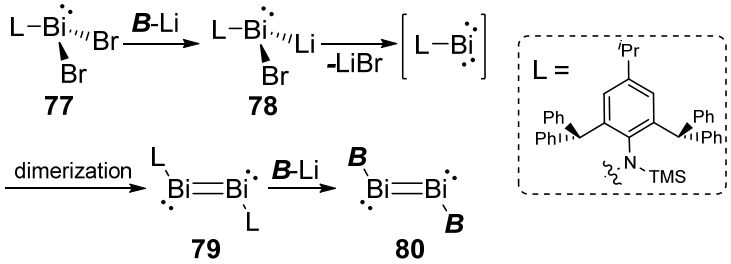

Scheme 1.15. Synthesis of boryl-substituted dibismuthene

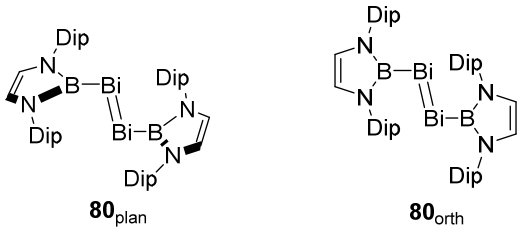

Figure 1.12. Structure of boryl-substituted dibismuthene

1.11 Structurally characterized phosphorus-centered radicals

Chemistry of phosphorus-center radical species is one of the most rapidly developing research areas.[35] Existence of phosphorus-centered radicals in chemical reaction were recognized for many decades, and simple phosphorus radicals were detected by ESR in solution. However, study of structural analysis of phosphorus-centered radical was just recently started due to high reactivity of phosphorus radicals. Power *et. al.* reported the gas-phase electron diffraction structure of phosphinyl radical **81** as the first structural data of phosphorus-centered radical. However, **81** had dimer-structure in the crystalline phase (Figure 1.13).[36]

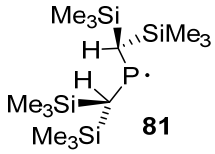

Figure 1.13. The first structural data of phosphorus-centered radical

After that, several reports have introduced isolation of phosphorus radical species by kinetic or thermodynamic stabilization. These radical compounds are broadly subdivided into three types, which are cationc,[37] neutral,[38] and anionic radical species.[39] Cation radicals of **82** to **86** are stabilized by carbenes, which are worked as strong electron donating ligands.

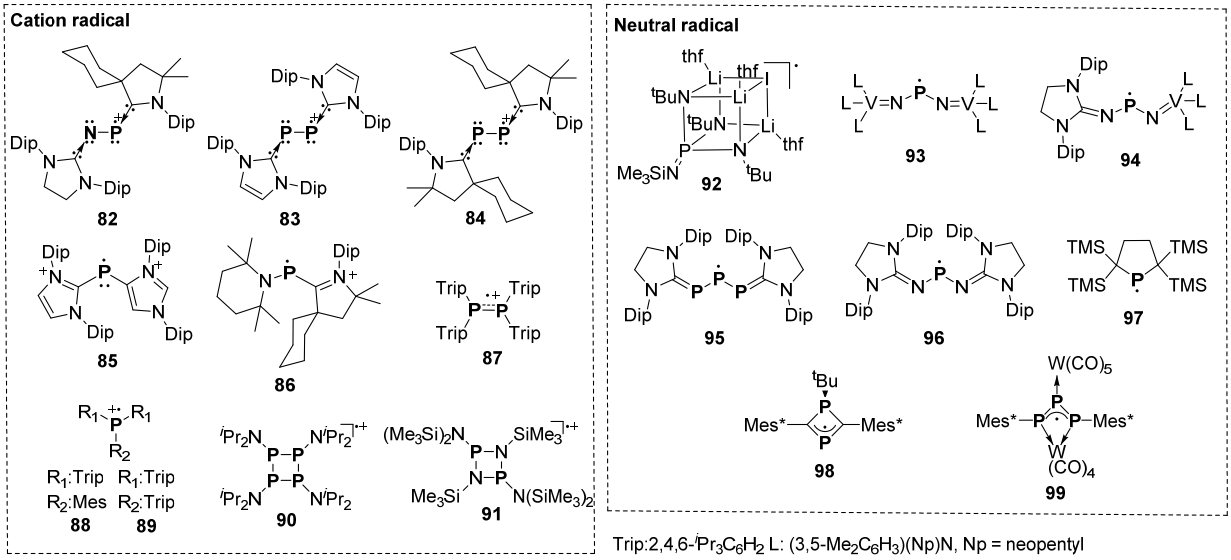

Figure 1.14. Structurally characterized cation and neutral phosphorus radicals

For example, one of resonance structures of bis(carbene)-P2 adduct **100** can be described as bis-phosphinidene moiety coordinated by two carbenes. (Scheme 1.11) Therefore, oxidation of **100** could proceed by using $Ph_3C^+B(C_6F_5)_4^-$ oxidation reaction, because of its having electron rich phosphorus.[37c] Therefore **83** evolved multi-bond character of P-P bonding. In the same manner, tetraaryldiphosphine radical cation of **87** has a shorter P-P length than typical P-P single bond.[37f]

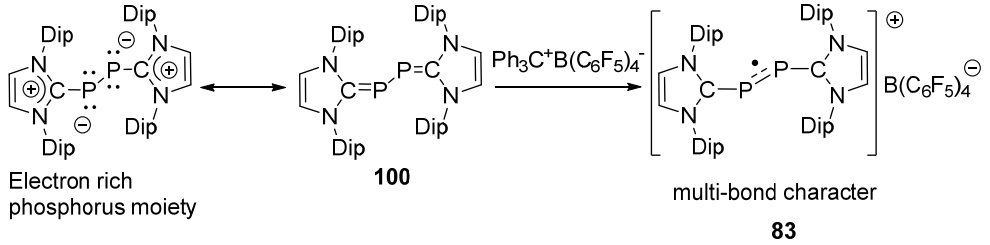

Scheme 1.16. Property of NHC-stabilized P2-radical cation

Triarylphosphine radical cations **88** and **89** show a relaxed pyramidal geometry of central phosphorus in comparison with those of neutral compounds. In addition, **89** displayed a perfectly planar geometry due to sterically hindered substituents and donation of the alkyl groups.[37e] Wang reported phosphorus-containing four-membering radical cations **90** and **91**.[37g] Almost spin densities of **90** reside on the exocyclic nitrogen atoms. However, spin densities of **90** delocalize mainly in P_2N_2 core by replacement of substituents with $SiMe_3$. These results revealed that exocyclic substituents affect spin distribution. For example of neutral radical, Chivers reported that [$Me_3SiNP(\mu_3\text{-}N^tBu)_3\{\mu_3\text{-}Li(thf)\}_3I$] **92** has a cubic structure by X-diffraction analysis, and that **92** is transformed into solvent-separated ion pair **101** in THF.[38a]

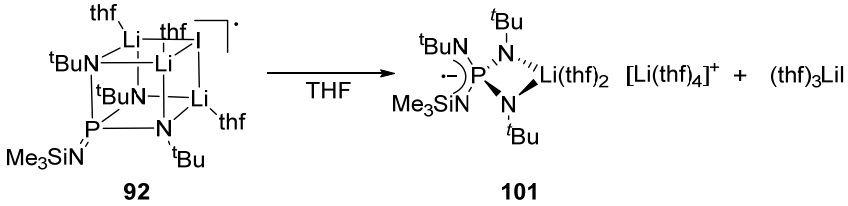

Scheme 1.17. Solvation of lithium ions in **91**

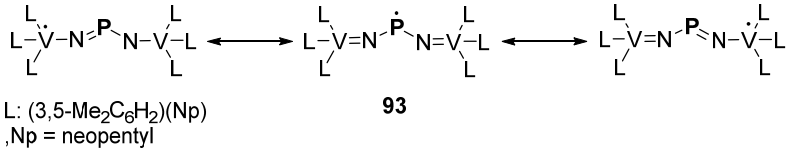

Scheme 1.18. Resonance structure of **93**

Cummins reported phosphorus-centered-radical **93**, which is stabilized by the vanadium (IV/V) redox couple.[38c] Orbital analysis revealed that **93** has only 31% of spin density in the 3p (P) orbital and about 23% over each vanadium atom. In the same manner, DFT calculations showed that **94** has almost spin density on the vanadium

center. While spin densities of NHC-stabilized neutral radicals **95** and **96** mainly delocalize in phosphorus center. Dialkylphosphinyl radical **97**, which has a helmet-shaped bidentate alkyl ligand, is monomeric form in solution and the solid state in contrast to **81**. **98** is stabilized by delocalization of neutral radical in a four membered 1,3-diphosphacyclobutenyl ring. Triphosphaallyl radical **99** have been resonance stabilized by the d orbitals of both W atoms.

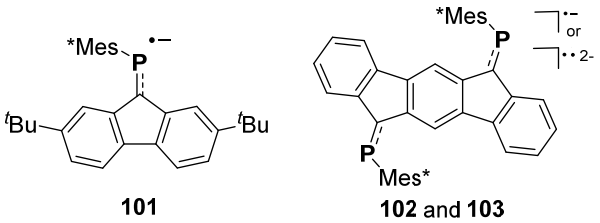

Figure 1.14. Structurally characterized anion phosphorus radicals

While phosphorus-centered radical anion, only three reports are available. Wang reported the structure of a phosphaalkene radical anions **101**, **102** and dianion **103**, in which the electron spin density mainly resides on the phosphorus atom. (Figure 1.14) In case of diphosphene radical anion, Tokitohs group isolated lithium diphosphene anion radicals by using 2,6-bis[bis(trimethylsilyl)methyl]-4-[tris(trimethylsilyl)methyl]phenyl group (Bbt) and 2,4,6-tris[bis(trimethylsilyl)methyl]phenyl (Tbt) as extremely bulky substituents.[11d] However, these compounds have not been structurally characterized by X-ray crystallographic analysis.

1.12 Synthesis of diphosphanediide

1,2-Dianion species, in which two negative charges are located on adjacent atoms, have become increasingly popular in organic synthesis. Diphosphanediide species have been known to be generated by reduction cyclooligophosphane or organophosphorus halides with alkali metals.[40] Recently, Grützmacher reported the crystal structure of two diphosphanediide. Disodium 1,2-diphenyldiphosphane-1,2-diide are detected as a cluster type structure **104**, which are prepared from reduction of $PhPCl_2$ with Na. In case of reduction $(PhP)_5$ with lithium in THF, $Li_2(P_2Ph_2)(thf)x$ was given as red powder. Subsequently, $Li_2(P_2Ph_2)(tmeda)_2$ **105** was obtained from recrystallization of toluene/TMEDA. Although diphosphene has been known to undergo one-electron reduction by alkali metal, generation of diphosphanediide have not been reported.

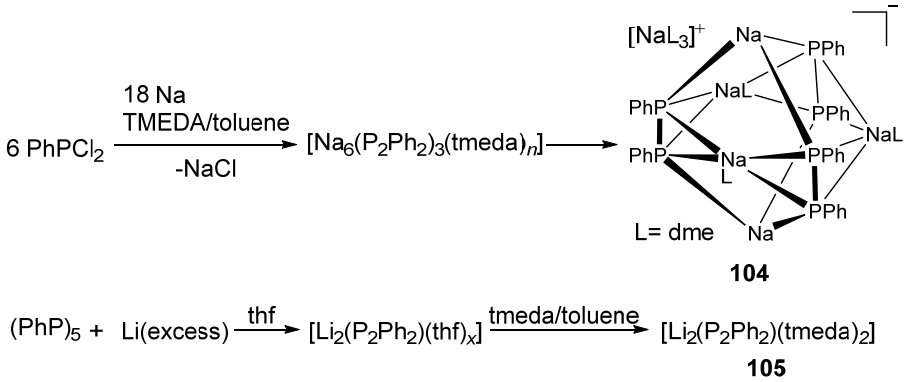

Scheme 1.19. Synthesis of diphosphanediide

1.13 1,3-Butadiene derivatives including heavier group elements

Direct connection of such heavy double bond has been known to lead to longer-wavelength shifted absorption. In the group 14 species, tetrasilabutadiene **106**[41] and tetragermabutadiene **107**[42] were reported to exhibit an absorption over 500 nm. Although the corresponding consecutive double bond species involving heavier group 15 element has never been reported, a reaction of $CpRh(CO)_2$ with P_4 was reported to give a dinuclear Rh complex possessing a dianionic tetraphosphabutadienediide ligand **108**.[43] While butadiene derivative incorporating less than four phosphorus atoms have been extensively studied since the first 2,3-diphospha-1,3-butadiene **109** was reported.[44] The isomeric 1,4-diphospha-1,3-butadiene species **110** has also been investigated and applied as a ligand to transition metal complexes.[45] As a similar species, Bertrand reported that CAAC [cyclic(alkyl)(amino)carbenes]-coordinated diphosphorus species[46] **111** has 2,3-diphospha-1,3-butadiene character in contrast to the case of NHC (N-heteocyclic carbene)-coordinated diphosphorus species **112**,[47] because of the stronger π-acceptor property of CAACs than those of NHCs.

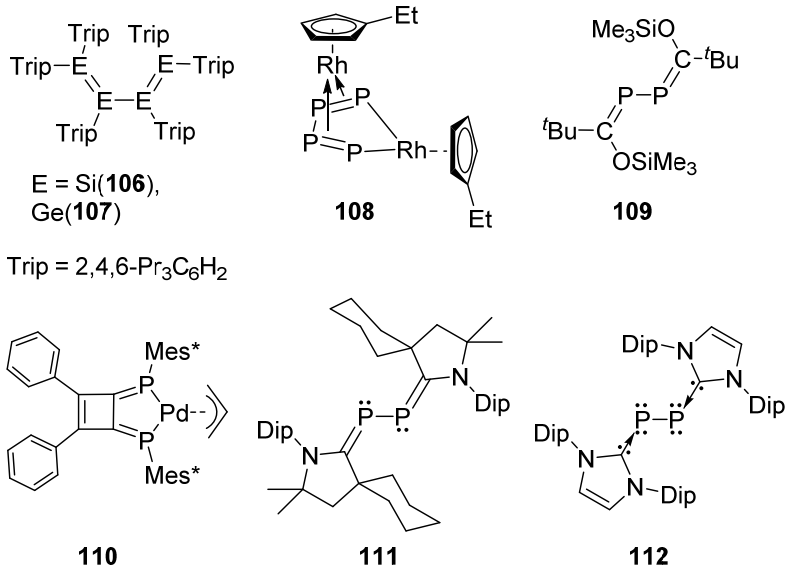

Scheme 1.20. 1,3-Butadiene derivatives including heavier group elements

1.14 Natural bond orbital analysis

NBO (Natural Bond Orbital) analysis[47] was developed as a technique for studying hybridization bond covalency effects in polyatomic wave function, based on local block eigenvectors of the one-particle density matrix. NBO has also enabled to describe corresponding closely to the picture of localized bonds and lone pairs as basic units of molecular structure. NBO have also been carried out by considering all interactions between filled donor and empty acceptor NBOs and estimating their energetic importance by second-order perturbation theory. The author described the interaction between a filled σ-orbital of the formal Lewis structure with one of the unfilled antibonding orbitals σ∗ to give the second-order energy lowering, $\Delta E^{(2)}_{\sigma\sigma^*}$ (Figure 1.15).

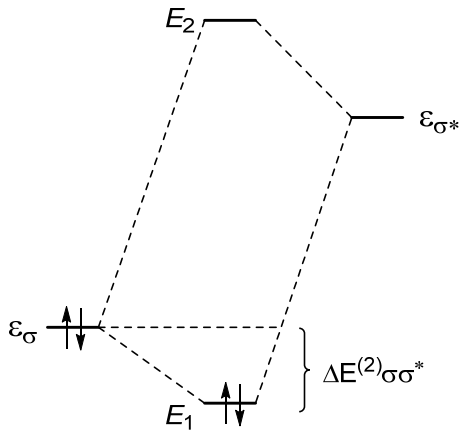

Figure 1.15. Perturbative donor-acceptor interaction, involving a filled orbital σ and an unfilled orbital σ*

This energy lowering is given by the formula (1) where $\hat{F}$ is the Fock operator and ε_σ and $\varepsilon_{\sigma*}$ are NBO orbital energies.

$$\Delta E^{(2)} = -2\frac{\langle\sigma|\hat{F}|\sigma^*\rangle^2}{\varepsilon_{\sigma*}-\varepsilon_\sigma} \quad (1)$$

1.15 The purpose of this thesis

As mentioned in the previous sections of this chapter, diphosphene species have been attracted by its structural, optical, and electronic property. These properties have been affected by substituents on the diphosphene. While boryl-substituents show some characteristic properties, which work as σ donor and π acceptor. For example, phosphino-borane and boryl-phosphide compound have pπ-pπ interaction between boron and phosphorus. The author expected that introduction of π-acceptor substituent to P=P double bond could affected property of diphosphene. Moreover, since the first reduction reaction of diphosphene was reported in 1982, structural characterization of diphosphene radical anion has never been reported. Although π-acceptor property of boryl substituent was anticipated to stabilize such as anionic species, there have been no reports of the synthesis of boryl-substituted diphosphene. Because the synthesis of boryl-dihalophosphine as a precursor has been difficult by using electrophilic boron reagent. Thus the author planned to synthesize diboryldiphosphene by the nucleophilic borylation method and investigated its property in this thesis. In chapter 2, synthesis of diboryldiphosphene, detail of property, and DFT calculations have been described. In particular, the author confirms boryl substituent has worked on σ-donor on diphosphene by means of comparison with HOMO and LUMO level of diboryldiphosphene, diphenyldiphophene as a model compound, and Mes*P=PMes*. In addition, the reaction of this diboryldiphosphene with ^{n}BuLi afforded a boryl-substituted phosphinophosphide that was stabilized by a π-electron-accepting effect of the boryl substituent in comparison with the thermally unstable Mes*-substituted derivative, In chapter 3, synthesis of diborydiphosphene radical anion species and characterization are described. X-ray structure of diboryldiphosphene radical anions have shown pπ-pπ interaction between boron and phosphorus, where result also has been supported by ESR spectroscopy and DFT calculations. In chapter 4, the author has revealed property of boryl-substituted diphosphanediide, which

was generated by the reaction of diboryldiphosphene with excess amount of lithium, from the NMR spectra, X-ray structure and reactivity toward MeI. Moreover, boryl-substituted diphosphanediide DMAP complex has been revealed to have 1,4-diboranuida-2,3-diphosphabutadiene (B^-=P-P=B^-) character by its X-ray and DFT calculation. In chapter 5, the final chapter of this dissertation, a conclusion throughout this study as well as perspectives of this chemistry in this thesis have been described.

Reference

(1) Power, P. P. *J. Chem. Soc. Dalton Trans*. **1998,** 2939.

(2) Kohler, H.; Michaelis, A. *Ber. Dtsch. Chem. Ges.* **1877**, *10*, 807.

(3) Daly, J. J. *J. Chem. Soc.* **1964,** 6147.

(4) West, R.; Fink, M. J.; Michl, J. *Science* **1981,** *214*, 1343-1344.

(5) Yoshifuji, M.; Shima, I.; Inamoto, N.; Hirotsu, K.; Higuchi, T. *J. Am. Chem. Soc.* **1981,** *103*, 4587.

(6) De Lange, J. J.; Monteath Robertson, J.; Woodward, I. *Proceedings of the Royal Society of London. Series A, Mathematical and Physical Sciences*, **1939,** *171*, 398.

(7) Shriver, D. F.; Atkins, P. W. *Inorganic Chemistry*, 4th ed. Oxford University Press, Oxford, U.K.

(8) Cowley, A. H.; Norman, N. C. *Progr. Inorg. Chem.* **1986,** *34*, 1.

(9) Ito, K.; Nagase, S. *Chem. Phys. Lett.* **1986,** *126*, 531.

(10) Bard, A. J.; Cowley, A. H.; Kilduff, J. E.; Leland, J. K.; Norman, N. C.; Pakulski, M.; Heath, G. A. *J. Chem. Soc. Dalton Trans.* **1987,** 249.

(11)(a) Cetinkaya, B.; Hudson, A.; Lappert, M. F.; Goldwhite, H.; *J. Chem. Soc. Chem. Commun.* **1982,** 609. (b) Culcasi, M.; Gronchi, G.; Escudié, J.; Couret, C.; Pujol, L.; Tordo, P.; *J. Am. Chem. Soc.* **1986,** *108*, 3130-3132. (c) Shah, S.; Burdette, S. C.; Swavey, S.; Urbach, F. L.; Protasiewicz, J. D.; *Organometallics* **1997,** *16*, 3395. (d) Sasamori, T.; Mieda, E.; Nagahora, N.; Sato, K.; Shiomi, D.; Takui, T.; Hosoi, Y.; Furukawa, Y.; Takagi, N.; Nagase, S.; Tokitoh, N.; *J. Am. Chem. Soc.* **2006,** *128*, 12582. (e) Nagahora, N.; Sasamori, T.; Hosoi, Y.; Furukawa, Y.; Tokitoh, N. *J. Organomet. Chem.* **2008,** *693*, 625-632.

(12) Markovski, L. N.; Romanenko, V. D.; Ruban, A. V. *Chemistry of Acyclic Compounds of Two-coordinated Phosphorus;* Naukova Dumka: Kiev, 1988 p 199.

(13) (a) Niecke, E.; Rüger, R. *Angew. Chem. Int. Ed. Engl.* **1983,** *22*, 155. (b) Niecke, E.; Rüger, R.; Lysek, M.; Pohl, S.; Schoeller, W. W. *Angew. Chem. Int. Ed. Engl.* **1983,** *22*, 486.

(14) Nagahora, N.; Sasamori, T.; Takeda, N. Tokitoh, N. *Chem. Eur. J.* **2004,** *10*, 6146.

(15) (a) Cowley, A. H.; Kilduff, J. E.; Norman, N. C.; Pakulski, M. *J. Chem. Soc. Dalton. Trans*. **1986,** 1801. (b) Cowley, A. H.; Pakulski, M. *J. Am. Chem. Soc.* **1984,** *106*, 1491.

(16) Yoshifuji, M.; Shibayama, K.; Inamoto, N. *Chem. Lett.* **1984,** 115.

(17) Ito, S.; Okabe, S.; Ueta, Y.; Mikami, K. *Chem. Commun.* **2014,** *50*, 9204.

(18) (a) de Graaf, W.; Boersma, J.; Smeets, W. J. J.; Spek, A. L.; van Koten, G. *Organometallics* **1989,** *8*, 2907. (b) Onozawa, S.; Hatanaka, Y.; Sakakura, T.; Shimada, S.; Tanaka, M. *Organometallics* **1996,** *15*, 5450. (c) Tanaka, Y.; Yamashita, H.; Shimada, S.; Tanaka, M. *Organometallics* **1997,** *16*, 3246.

(19) Zhu, J.; Lin, Z.; Marder, T. B. *Inorg. Chem.* **2005,** *44*, 9384.

(20) (a) Dewar, M. J. S.; Rona, P. *J. Am. Chem. Soc.* **1969,** *91*, 2259. (b) Paine, R. T.; Nöth, H. *Chem. Rev.* **1995,** *95*, 343. (c) Power, P. P. *Chem. Rev.* **1999,** *99*, 3463.

(21) Burg, A. B.; Wagner, R. I. *J. Am. Chem. Soc.* **1953,** *16*, 3872.

(22) Goldstein, P.; Jacobson, R. A. *J. Am. Chem. Soc.* **1962,** *84*, 2457.

(23) (a) Olmstead, M. M.; Power, P. P. *J. Am. Chem. Soc.* **1986,** *108*, 4235. (b) Pestana, D. C.; Power, P. P. *J. Am. Chem. Soc.* **1991,** *113*, 8426. (c) Bryan, P. S.; Kuczkowski, R. L. *Inorg. Chem.*, **1972,** *11*, 553.

(24) (a) Segawa, Y.; Yamashita, M.; Nozaki, K., *Science* **2006,** *314*, 113. (b) Segawa, Y.; Yamashita, M.; Nozaki, K. *Angew. Chem. Int. Ed.* **2007,** *46*, 6710. (c) Yamashita, M.; Suzuki, Y.; Segawa, Y.; Nozaki, K., *J. Am. Chem. Soc.* **2007,** *129*, 9570. (d) Segawa, Y.; Suzuki, Y.; Yamashita, M.; Nozaki, K., *J. Am. Chem. Soc.* **2008,** *130*, 16069. (e) Yamashita, M.; Nozaki, K., *Bull. Chem. Soc. Jpn.* **2008,** *81*, 1377. (f) Yamashita, M.; Suzuki, Y.; Segawa, Y.; Nozaki, K., *Chem. Lett.* **2008,** *37*, 802. (g) Terabayashi, T.; Kajiwara, T.; Yamashita, M.; Nozaki, K., *J. Am. Chem. Soc.* **2009,** *131*, 14162. (h) Nozaki, K.; Aramaki, Y.; Yamashita, M.; Ueng, S.-H.; Malacria, M.; Lacôte, E.; Curran, D. P. *J. Am. Chem. Soc.* **2010,** *132*, 11449. (i) Hayashi, Y.; Segawa, Y.; Yamashita, M.; Nozaki, K. *Chem. Commun.* **2011,** *47*, 5888. (j) Okuno, Y.; Yamashita, M.; Nozaki, K. *Angew. Chem. Int. Ed.* **2011,** *50*, 920. (k) Okuno, Y.; Yamashita, M.; Nozaki, K. *Eur. J. Org. Chem.* **2011,** *2011*, 3951. (l) Yamashita, M. *Bull. Chem. Soc. Jpn.* **2011,** *84*, 983. (m) Dettenrieder, N.; Aramaki, Y.; Wolf, B. M.; Maichle-Mössmer, C.; Zhao, X.; Yamashita, M.; Nozaki, K.; Anwander, R. *Angew. Chem. Int. Ed.* **2014,** *53*, 6259. (n) Yamashita, M.; Nozaki, K. Boryl Anions. In *Synthesis and Application of Organoboron Compounds*, Fernández, E.; Whiting, A., Eds. Springer International Publishing: 2015; pp 1-37. (o) Kisu, H.; Sakaino, H.; Ito, F.; Yamashita, M.; Nozaki, K. *J. Am. Chem. Soc.* **2016,** *138*, 3548. (p) Ohsato, T.; Okuno, Y.; Ishida, S.; Iwamoto, T.; Lee, K.-H.; Lin, Z.; Yamashita, M.; Nozaki, K. *Angew. Chem. Int. Ed.* **2016,** *55*, 11426. (q) Asami, S.-s.; Okamoto, M.; Suzuki, K.; Yamashita, M. *Angew. Chem. Int. Ed.* **2016,** *55*, 12827.

(25) Protchenko, A.V. Birjkumar, K. H. Dange, D. Schwarz, A. D. Vidovic, D. Jones, C. Kaltsoyannis, N. Mountford, P. Aldridge, S. *J Am Chem Soc* **2012,** *134*, 6500.

(26) Protchenko, A.V.; Dange, D.; Schwarz, A.D.; Tang, C.Y.; Phillips, N.; Mountford, P.; Jones, C. Aldridge, S. *Chem. Commun.* **2014,** *50*, 3841.

(27) Protchenko, A.V.; Dange, D.; Harmer, J. R.; Tang, C. Y.; Schwarz, A. D.; Kelly, M. J.; Phillips, N.; Tirfoin, R.; Birjkumar, K. H.; Jones, C.; Kaltsoyannis, N.; Mountford, P.; Aldridge, S. *Nat. Chem.* **2014,** *6*, 315.

(28) Kaaz, M.; Bender, J.; Forster, D.; Frey, W.; Nieger, M.; Gudat, D. *Dalton Trans.* **2014,** *43*, 680.

(29) Wei, L.；Haitao, H.；Yongxin, L.；Rakesh, G.；Kinjo, R. *J. Am. Chem. Soc.*, **2016,** *138*, 6650.

(30) Inoue, S.; Ichinohe, M.; Sekiguchi, A. *Chem. Lett.* **2008,** *37*, 1044.

(31) (a) Takeuchi, K.; Ikoshi, M.; Ichinohe, M.; Sekiguchi, A. *J. Am. Chem. Soc.* **2010,** *132*, 930. (b) Takeuchi, K.; Ichinohe, M.; Sekiguchi, A. *Organometallics* **2011,** *30*, 2044.

(32) Rit, A.; Campos, J.; Niu, H.; Aldridge S. *Nat. Chem.* **8,** 1022.

(33) Green, A. P.; Jones, C.; Stasch, A. *Science* **2007,** 318, 1754.

(34) Dange, D.; Davey, A.; Abdalla, J. A. B.; Aldridge, S.; Jones, C. *Chem. Commun.* **2015,** *51*, 7128.

(35) (a) Power, P. P. *Chem. Rev.* **2003,** *103*, 789. (b) Leca, D.; Fensterbank, L.; Lacôte, E.; Malacria, M. *Chem. Soc. Rev.* **2005,** *34*, 858.

(36) (a) Hinchley, S. L.; Morrison, C. A.; Rankin, D. W. H.; Macdonald, C. L. B.; Wiacek, R. J.; Cowley, A. H.; Lappert, M. F.; Gundersen, G.; Clyburne, J. A. C.; Power, P. P. *Chem. Commun.* **2000,** 2045. (b) Hinchley, S. L.; Morrison, C. A.; Rankin, D. W. H.; Macdonald, C. L. B.; Wiacek, R. J.; Voigt, A.; Cowley, A. H.; Lappert, M. F.; Gundersen, G.; Clyburne, J. A. C.; Power, P. P. *J. Am. Chem. Soc.* **2001,** *123,* 9045.
(37) (a) Scheer, M.; Kuntz, C.; Stubenhofer, M.; Linseis, M.; Winter, R. F.; Sierka, M. *Angew. Chem. Int. Ed.* **2009,** *48,* 2600. (b) Back, O.; Celik, M. A.; Frenking, G.; Melaimi, M.; Donnadieu, B.; Bertrand, G. *J. Am. Chem. Soc.* **2010,** *132,* 10262. (c) Back, O.; Donnadieu, B.; Parameswaran, P.; Frenking, G.; Bertrand, G. *Nature Chem.* **2010,** *2,* 369. (d) Kinjo, R.; Donnadieu, B.; Bertrand, G. *Angew. Chem. Int. Ed.* **2010,** *49,* 5930. (e) Pan, X.; Chen, X.; Li, T.; Li, Y.; Wang, X. *J. Am. Chem. Soc.* **2013,** *135,* 3414. (f) Pan, X.; Su, Y.; Chen, X.; Zhao, Y.; Li, Y.; Zuo, J.; Wang, X. *J. Am. Chem. Soc.* **2013,** *135,* 5561. (g) Su, Y.; Zheng, X.; Wang, X.; Zhang, X.; Sui, Y.; Wang, X. *J. Am. Chem. Soc.* **2014,** *136,* 6251. (h) Schwedtmann, K.; Schulz, S.; Hennersdorf, F.; Strassner, T.; Dmitrieva, E.; Weigand, J. J.; *Angew. Chem. Int. Ed.* **2015,** *54,* 11054.
(38) (a) Armstrong, A.; Chivers, T.; Parvez, M.; Boeré, R. *Angew. Chem. Int. Ed.* **2004,** *123,* 502. (b) Ito, S.; Kikuchi, M.; Yoshifuji, M.; Arduengo, A. J. III.; Konovalova, T. A.; Kispert, L. D. *Angew. Chem. Int. Ed.* **2006,** *45,* 4341. (c) Agarwal, P.; Piro, N. A.; Meyer, K.; Müller, P.; Cummins, C. *Angew. Chem. Int. Ed.* **2007,** *46,* 3111. (d) Back, O.; Donnadieu, B.; von Hopffgarten, M.; Klein, S.; Tonner, R.; Frenking, G.; Bertrand, G. *Chem. Sci.* **2011,** *2,* 858-861. (e) Ishida, S.; Hirakawa, F.; Iwamoto, T. *J. Am. Chem. Soc.* **2011,** *133,* 12968. (f) Tondreau, A. M.; Benkő, Z.; Harmer, J. R.; Grützmacher, H. *Chem. Sci.* **2014,** *5,* 1545.
(39) (a) Pan. X.; Wang. X.; Zhao, Y.; Sui. Y.; Wang. X. *J. Am. Chem. Soc.* **2014**, *136*, 9834-9837. (b) Tan, G.; Li, S.; Chen, S.; Sui, Y.; Zhao, Y.; Wang, X. *J. Am. Chem. Soc.* **2016,** *138*, 6735.
(40) (a) Issleib, K.; Krech, K. *Chem. Ber.* **1966,** *99,* 1310. (b) Hoffman, P. R.; Caulton, K. G. *J. Am. Chem. Soc.* **1975**, 97, 6370. (c) Reesor, J. W. B.; Wright, G. F. *J. Org. Chem.* **1957,** *22*, 385. (d) Baudler, M.; Gruner, C.; Fürstenberg, G.; Kloth, B.; Sayokowski, F.; Özer, U. *Anorg. Allg. Chem.* **1978,** *446*, 169. (e) Geier, J.; Rüegger, H.; Flock, M.; Grützmacher, H. *Angew. Chem. Int. Ed.* **2003,** *42*, 3951. (f) Stein, D.; Dransfeld, A.; Flock, M.; Rüegger, H.; Grützmacher, H. *Eur. J. Inorg. Chem.* **2006,** 4157.
(41) Weidenbruch, M.; Willms, S.; Saak, W.; Henkel, G. *Angew. Chem. Int. Ed.* **1997,** *36,* 2503.
(42) Schäfer, H.; Saak, W.; Weidenbruch, M. *Angew. Chem. Int. Ed.* **2000,** *39,* 3703.
(43) Scherer, O. J.; Swarowsky, M. *Angew. Chem. Int. Ed.* **1998,** *27,* 694.
(44) (a) Toyota, K.; Tashiro, K.; Yoshifuji, M. *Chem. Lett.* **1991,** 2079. (b) Toyota, K.; Tashiro, K.; Yoshifuji, M. *J. Organomet. Chem.* **1992,** *431,* C35. (c) Yoshifuji, M.; Ichikawa, Y. Toyota, K.; Kasashima, E.; Okamoto, Y. *Chem. Lett.* **1997,** 87. (d) Yoshifuji, M.; Ichikawa, Y.; Yamada, N.; Toyota, K. *Chem. Commun.* **1998,** 27. (e) Tatsuya, M.; Okamoto, H.; Ikeda, S.; Tanaka, R.; Ozawa, F.; Yoshifuji, M. *Angew. Chem. Int. Ed.* **2001,** *40,* 4501.
(45) (a) Appel, R.; Barth, V.; Knoch, F. *Chem. Ber.* **1983,** *116,* 938. (b) Appel, R.; Kgndgen, U.; Knoch, F.; *Chem. Ber.* **1985,** *118,* 1352. (c) Romanenko, V. D.; Kachkovskaya, L. S.; Markovskii, L. N.; *Zh. Obshch. Khim.* **1985,** *55,* 2140. (c) Märkl, G.; Sejpka, H.; *Tetrahedron Lett.* **1986,** *27,* 171; (d) Markovskii, L. N.; Romanenko, V. D.; Kachkovskaya, L. S.; Povolotskii, M. I.; Patsanovskii, I. I.; Stepanova, Yu. Z.; Ishmaeva, E. A. *Zh. Obshch. Khim.* **1987,** *57,* 901; (e) Breit, B.; Memmesheimer, H.; Boese, R.; Regitz, M. *Chem. Ber.* **1992,** *125,* 729. (f)

Seidl, M.; Stubenhofer, M.; Timoshkin, A. Y.; Scheer, M.; *Angew. Chem. Int. Ed.* **2016,** 55, 14037.
(46) Back, O.; Kuchenbeiser, G.; Donnadieu, B.; Bertrand, G. *Angew. Chem. Int. Ed.* **2009,** *48*, 5530.; *Angew. Chem.* **2009,** *121*, 5638.
(47) Wang, Y.; Xie, Y.; Wie, P.; King, R. B.; Schaefer, H. F.; Schleyer, P.； von R.; Robinson, G. H. *J. Am. Chem. Soc.* **2008,** *130*, 14970.
(48) Reed, A. E.; Curtiss, L. A.; Weinhold, F. *Chem. Rev.* **1988,** 88, 899.

Chapter 2

A Boryl-Substituted Diphosphene: Synthesis, Structure, and Reactivity with ^{n}BuLi to Form An Isolable Adduct Stabilized by pπ-pπ Interactions

2.1, Introduction

The synthesis and photophysical properties of boron-containing organic molecules have been thoroughly investigated [1] especially with respect to the substituent effects of the boryl group. The π-acceptor properties of boryl substituents are due to a vacant p-orbital, which may accept electrons from adjacent atoms. (Chapter 1.6) But boryl substituents also exhibit strong σ-donor properties due to the relatively low electronegativity of the second-row element boron atom (2.04, Pauling), which is reflected in e.g. the strong *trans*-influence of boryl ligands in transition-metal-boryl complexes (Chapter 1.5). In contrast to the well-understood substituent effect of the boryl-substituent in organic and coordination chemistry, the effects in main group chemistry remain relatively unexplored, probably due to the limited availability of boryl-substituted main-group-element compounds. However, nucleophilic boryllithium has been utilized to make novel E-B bonds via nucleophilic borylation of electrophilic main group reagents. (Chapter 1.8) (E = B, Al, Ga, In, TI, C, Si, Ge, Sn, and P) Aldridge reported interesting redox chemistry at the main group elements, e.g. direct reaction of borylsilylene with dihydrogen, or the formation of divalent group 13 radical species.[2] However, these studies on boryl anion-derived main-group-element compounds did not reveal any information regarding the substituent effect of boryl groups on the redox chemistry. The author described basic property of diphosphene in chapter 1. The properties of the P=P double bond are strongly influenced by the substituents on the phosphorus atoms. So far, aryl,[3a, b] alkyl,[4] silyl,[5] thio,[6] amino-substituted diphosphenes[7] have been reported (Figure 1). Although two computational studies on boryl-substituted diphosphenes have been reported,[8] such species have not yet been investigated experimentally.[9] Herein, the author reports the synthesis and property of a diboryldiphosphene. Characterization of this diphosphene by UV/Vis spectroscopy, cyclic voltammetry, and DFT calculations revealed that the boryl substituents act as σ-donor substituents. Moreover diboryldiphosphene reacts with ^{n}BuLi to furnish an isolable phosphinophosphide, which is stabilized by pπ–pπ interactions between the boron and the phosphorus atoms. This behavior is thus markedly different to that of the Mes*-substituted diarylphosphene **9**.

2.2, Results and discussions

2.2.1, Synthesis of diboryldiphosphene 113

The author used to precursor as chloroborane **114** possessing a saturated C-C bond because aromaticity of **37** may reduce π-acceptor property of boryl-substituent. Previously, it was reported that the reaction of boryllithium with PCl_3 generated the corresponding chloroborane, because of halogen abstraction reaction by boryllithium (Scheme 1).[10] Therefore, the transmetallation of the boryllithium **115**, which was prepared from **114**, with 1.2 equivalents of $ZnCl_2$ afforded THF-coordinated dimeric borylzinc chloride (**116**·thf)$_2$ via a procedure similar to that of previously reported borylzinc species (Scheme 2).[11] This direct substitution at the main group element with a nucleophilic borylzinc reagent stands in stark contrast to the reductive dehalogenation of aminodibromobismuthane(III), which is converted into a diborylbismuthene through a Bi(I) intermediate, reported by Jones *et al.* [12] The reaction of isolated (**116**·thf)$_2$ with PCl_3 in acetonitrile resulted in the formation of boryldichlorophosphine **117**. Additionally, the molecular structure of **117** has been determined by a single-crystal X-ray diffraction study (Figure 1). The observed B-P bond length of 1.952(2) Å in **117** is close to the sum of the covalent radii of the B and P atoms (1.98 Å),[13] which suggests the absence of any pπ- pπ interactions.

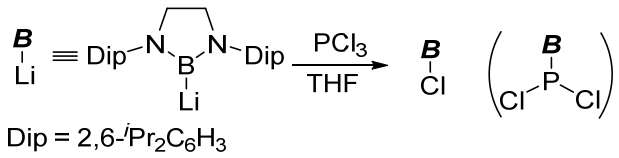

Scheme 1. Reaction of boryllithium with PCl_3

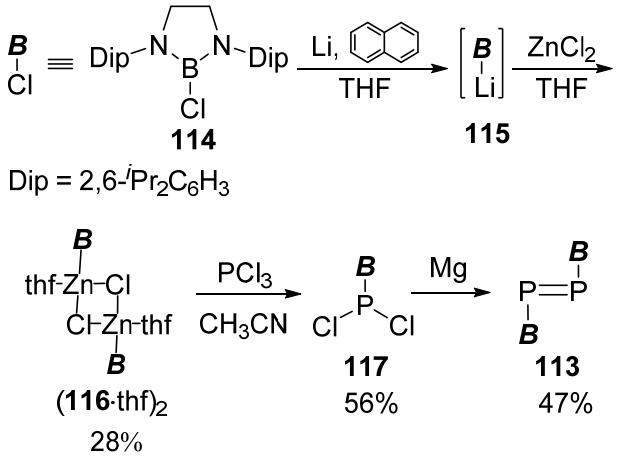

Scheme 2. Synthesis of diboryldiphosphene **113**

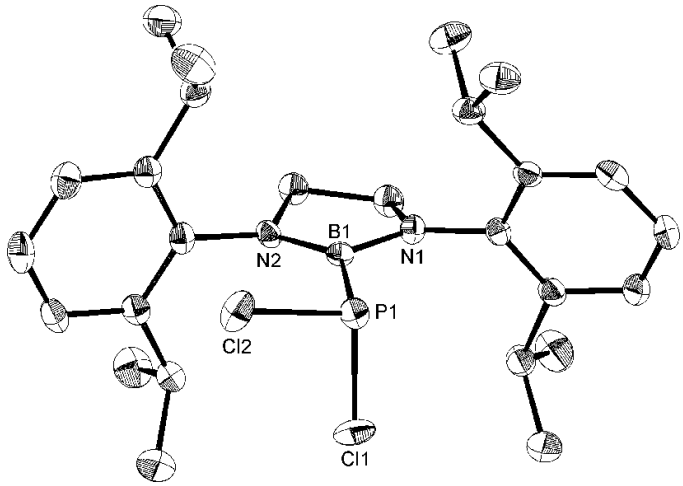

Figure 1. Crystal structure of **117** (thermal ellipsoid set a 50%, hydrogen atoms are omitted for clarity); Selected bond lengths [Å] and angles [º]: P1-B1 1.952(2), B1-N1 1.409(3), B1-N2 1.397(3), N2-B1-N1 110.32(17)

A subsequent reduction of **117** with magnesium in THF furnished diboryldiphosphene **113** in moderate yield. In the ^{31}P NMR spectrum of **113** in C_6D_6, two magnetically equivalent phosphorus nuclei were observed at δ_P 605 ppm, which are comparable, albeit slightly low-field-shifted, to the resonances of carbon-substituted symmetrical trans-diphosphenes (δ_p 477–600 ppm)[3a, 3b, 4, 1]. The electropositive boryl-substituents may contribute to the low-field shift of these resonances, considering that the chemical shifts of symmetrical diphosphenes with electropositive silyl substituents (electronegativity of Si: 1.90, Pauling) are further downfield-shifted (δ_p 735, 818 ppm) (Figure 2).[5c, 5d] The ^{11}B NMR spectrum of **113** showed a broad signal at δ_B

30 ppm.

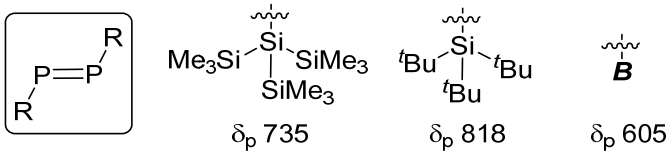

Figure 2. Comparison of ^{31}P NMR chemical shift between silyl-substituted diphosphene and **113**

2.2.2, Structure of diboryldiphosphene 113

The centrosymmetric molecular structure of **113** was determined by single-crystal X-ray diffraction analysis (Figure 3). The observed P=P bond length of 2.0655(17) Å is slightly longer than those of previously reported carbon-substituted diphosphene [1.985(3)[15]-2.051(2)[16] Å].The two boron containing planes are oriented almost perpendicular to the planar B-P=P-B moiety, exhibiting a dihedral N2-B1-P1-P1* angle of -83.2(2)º. This structure stands in stark contrast to the perpendicular and coplanar conformers that were observed for the recently reported diboryldibismuthene. The B1–P1 bond length of 1.936(3) Å in **113** is similar to the B-P bond length in **117** [1.952(2) Å], indicating a single-bond character for this bond, due to little overlap between the 2p and 3p orbitals of the boron and phosphorus atoms, respectively. The observed B1-P1-P1* angle of 95.83(9) Å is relatively small, but still within the range of the corresponding C-P-P angles of symmetrical carbon-substituted diphosphenes [93.22(5)º[17]-114.9(1)º[16]].

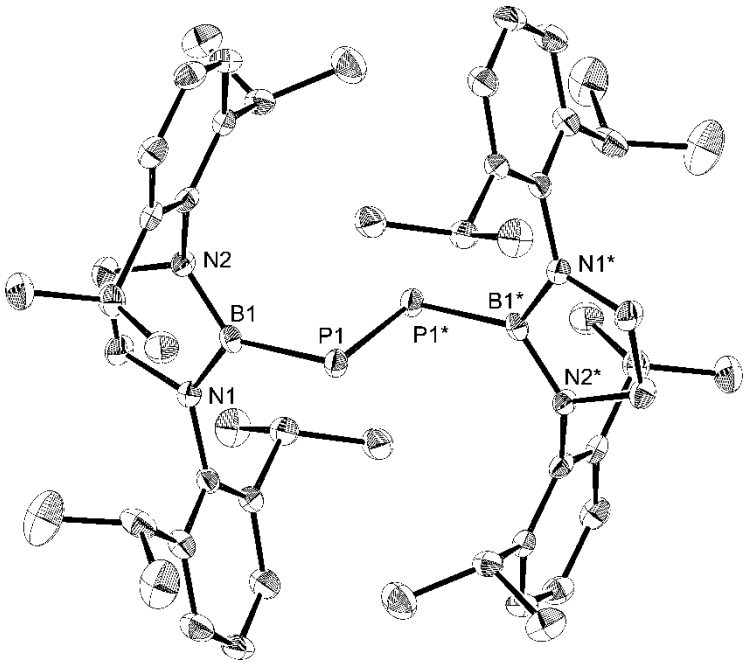

Figure 3. Crystal structure of **113** (thermal ellipsoid set at 50% probability hydrogen atoms omitted for clarity; asterisks denote atoms generated by symmetry operation), Selected bond lengths [Å] and angles [º]: P1-B1 1.934(3) , N1-B1 1.420(4), N2-B1 1.425(4), P1-P2 2.0661(18), N2-B1-N1 108.1(2), P1-P1-B1-N1 95.9(3)

2.2.3, DFT calculations of diboryldiphosphene 113

DFT calculations at the B3LYP/6-31G level of theory revealed the following features. By using the crystal structure as an initial geometry, the optimized structure of **113** was obtained with similar structural parameters [P=P 2.054 Å; B-P 1.966 Å; B-P-P 101.6°; N-B-P-P torsion angle -85.3°] and parallel relationship between two diazaborole rings. The resulting structure is named as **113**(85_*Ci*). In addition, NBO analysis of **113**(85_*Ci*) has shown that Wiberg bond indexes of B-P and P=P are 1.033 and 1.911, respectively. Moreover, small second-order perturbation energies are estimated to be 3.86 kcal/mol between boron and phosphorus in **113**. These results are in good agreement with small pπ-pπ interaction between boron and phosphorus. Selected molecular orbitals of **113**(85_C_i) are illustrated in Figure 5. (1) the HOMO exhibits features of the nonbonding lone pair on the phosphorus atoms [Figure 5(b)], (2) the HOMO-7 and the LUMO correspond to the π and π* orbitals of the P=P double bond [Figure 5(a), (d)], and (3) the HOMO-1 is predominantly characterized by contributions from the π-type orbital of the diazaborole moieties [Figure 5(c)].

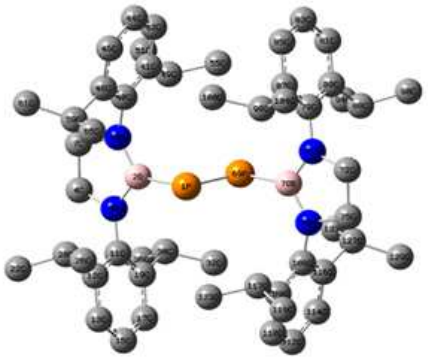

Wiberg bond index

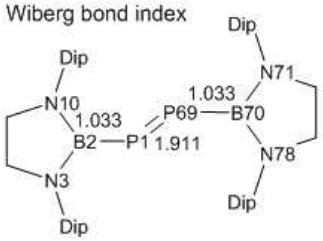

Second order perturbation energy (kcal/mol)

Donor	Acceptor	ΔE
LP (P1)	LP* (B2)	3.86
LP (P69)	LP* (B70)	3.86
LP (N3)	LP* (B2)	70.19
LP (N10)	LP* (B2)	67.76
LP (N71)	LP* (B70)	70.19
LP (N78)	LP* (B70)	67.76

Figure 4. The optimized structures of **113**(85_C_i) and results of NBO analysis

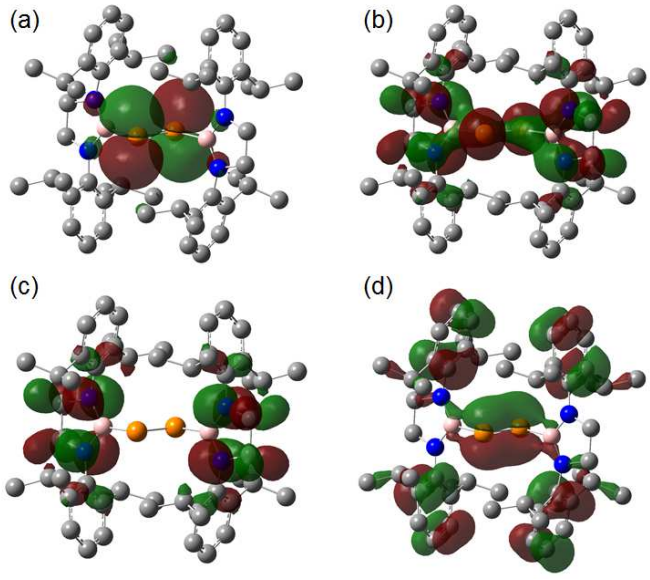

Figure 5. Selected molecular orbitals of **113**(85_C_i) calculated with B3LYP/6-31G(d) level [(a) LUMO, (b) HOMO, (c) HOMO-1, (d) HOMO-7] (hydrogen atoms are omitted for clarity, gray: carbon, blue: nitrogen, orange: phosphorus, pale peach: boron)

2.2.4, Optical and electronic properties of diboryldiphosphene 113

To better understand the electronic effects of the boryl-substituents in **113**, the compound was subjected to UV/Vis spectroscopy and cyclic voltammetry, and further DFT calculations. The UV/Vis spectrum of **113** showed two absorption maxima at 310 nm (ε=5700) and 400 nm (ε=680) (Figure 6), which were assigned as π-π* and n–π* transition by TD-DFT calculations (Figure 7). Two absorption maxima of **113** are slightly blue-shifted relative to the absorptions of Mes*-substituted diarylphosphene **9** (325, 460–532 nm),[3] indicating a larger HOMO–LUMO gap of **9** relative to that of **113**. The cyclic voltammogram of **2** in THF (supporting electrolyte: 0.100 M [^{n}Bu$_4$N][BF$_4$]) showed a reversible reduction wave at -2.24 V (vs. Cp_2Fe/Cp_2Fe^+; Figure 8), which is lower than that of **113** (-2.36 V),[18] suggesting a lower LUMO level in **113** relative to that in **9**. (vs. Cp_2Fe/Cp_2Fe^+; Figure 9)

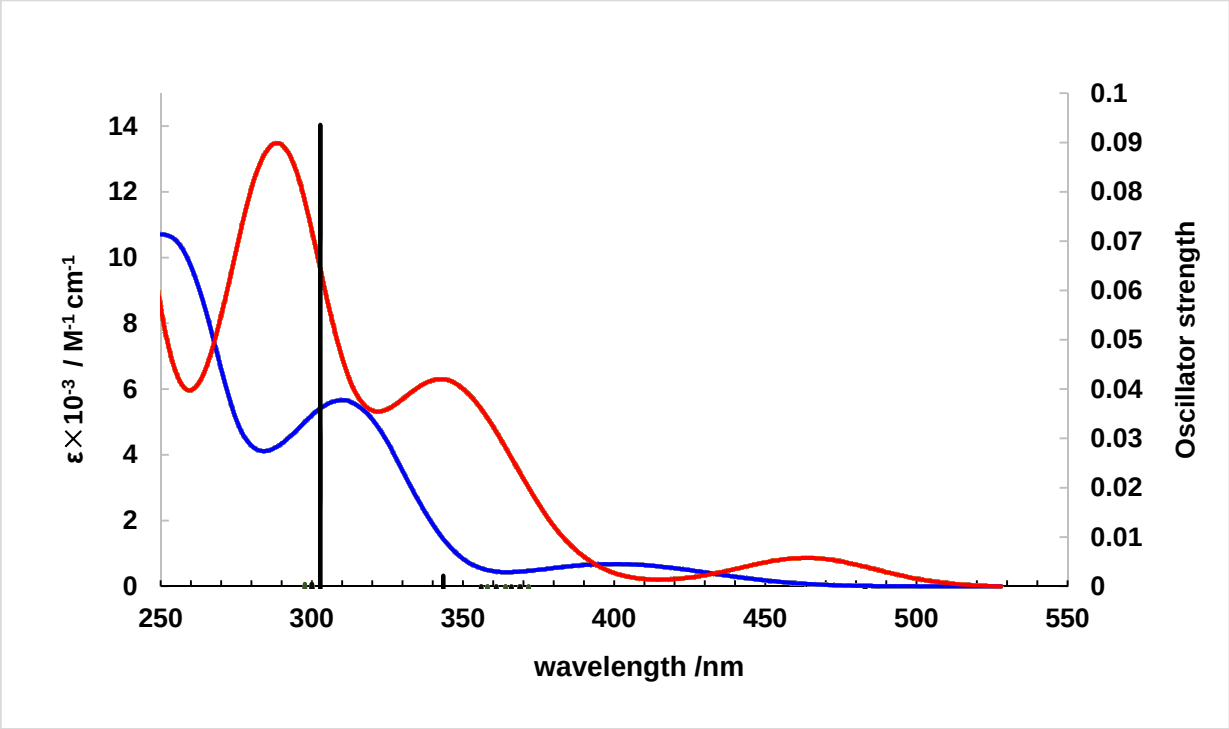

Figure 6. UV-vis spectra of **9** (blue), **113** (red), and **113** (black) at CAM-B3LYP/6-31G(d)

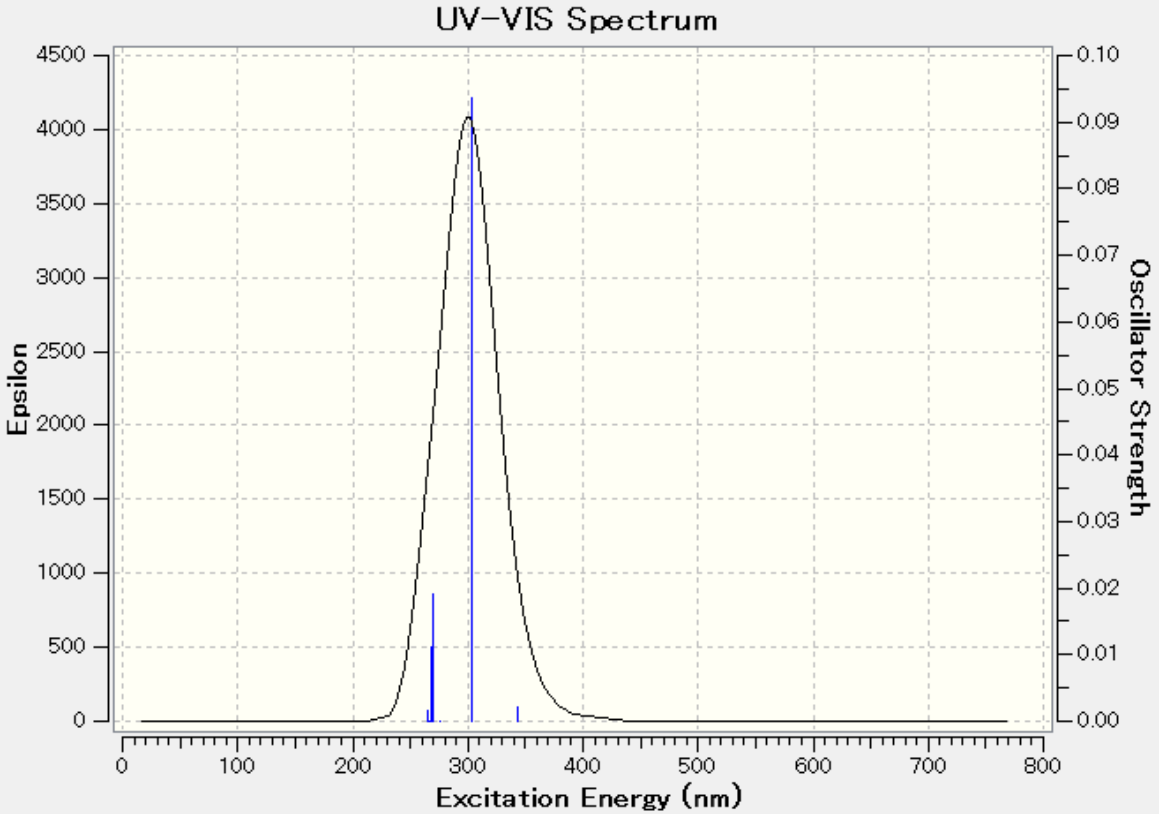

Figure 7. Simulated UV-vis spectrum of **113**(85_C_i) by TD-DFT calculations.

Table 1. Parameter of UV-vis spectrum of **113**(85_C_i) by TD-DFT calculations.

Excited State		Calculated	
1	HOMO→LUMO	519.41 nm	f = 0.0000
2	HOMO-1→LUMO	343.99 nm	f = 0.0010
4	HOMO-7→LUMO	302.82 nm	f = 0.0936
7	HOMO-9→LUMO	270.26 nm	f = 0.0190
8	HOMO-3→LUMO	267.96 nm	f = 0.0111

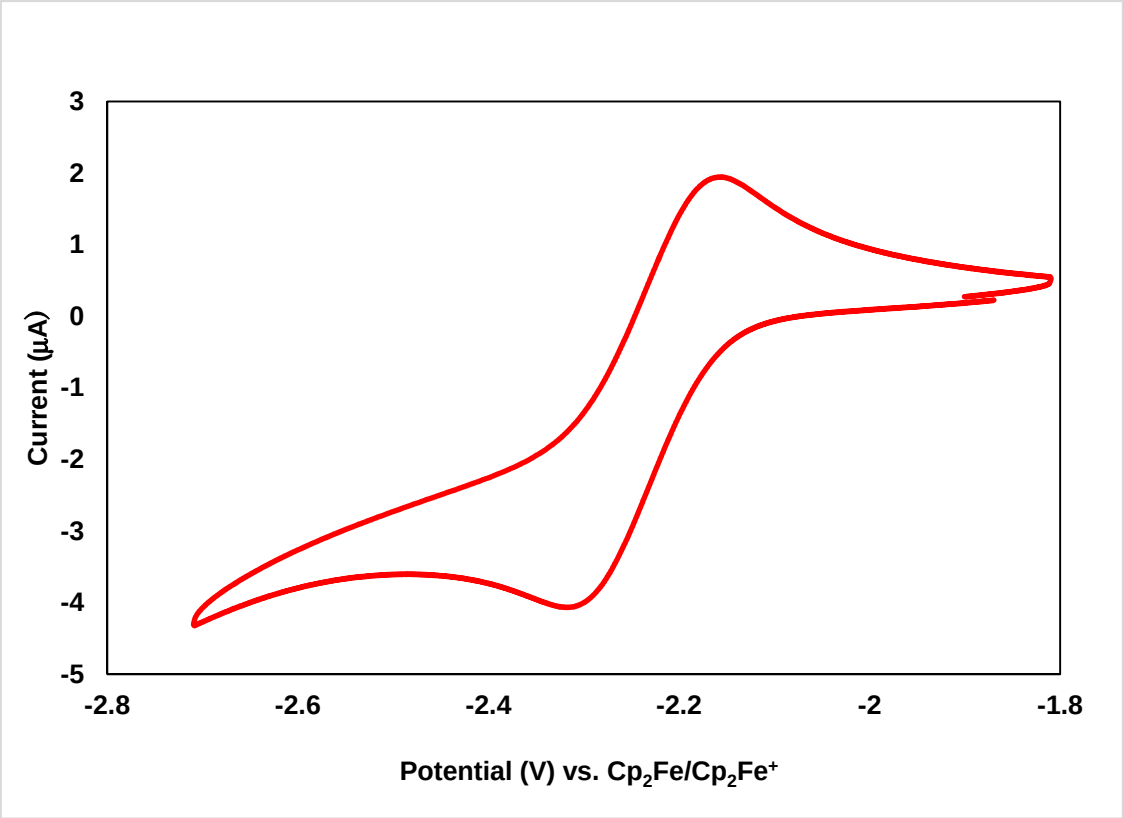

Figure 8. Cyclic voltammogram of a 0.100 mM solution of **113** in THF [electrolyte: $^{n}Bu_4NPF_6$ (0.100 M)]

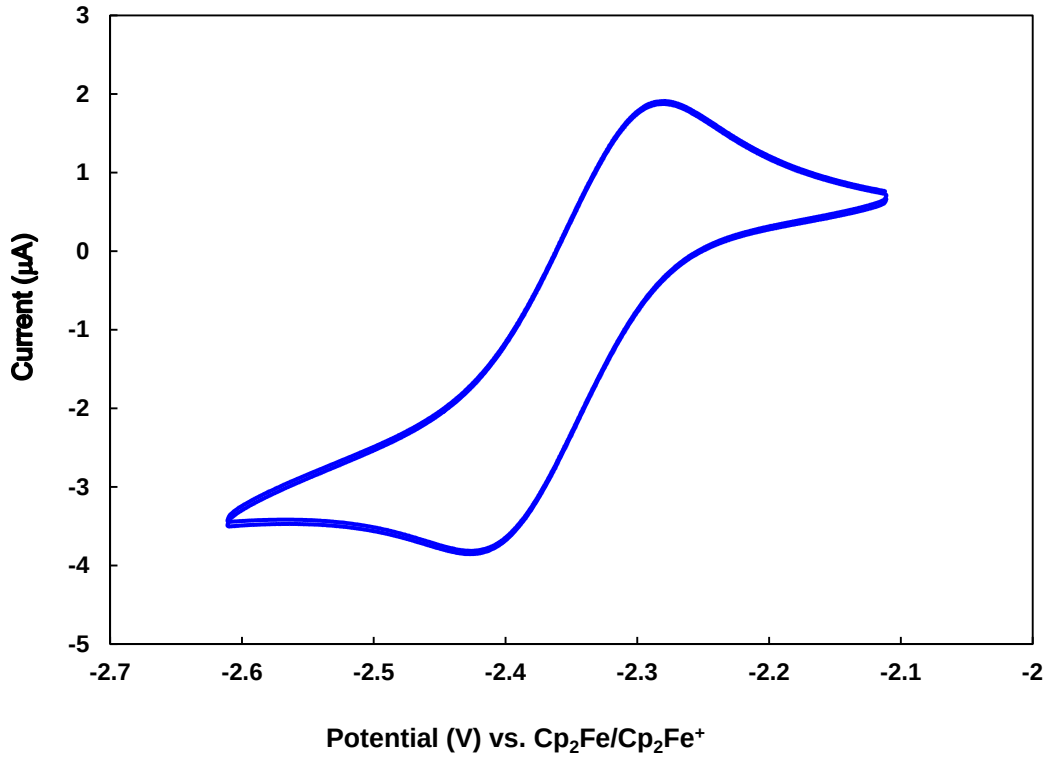

Figure 9. Cyclic voltammogram of a 0.01 M solution of **9** in THF [electrolyte: $^{n}Bu_4NPF_6$ (0.100 M)]

2.2.5, The influence of boryl-substituent on P=P double bond

The author confirmed properties of boryl-substituent by means of comparison with HOMO and LUMO levels of diboryldiphosphene **113**, diphenyldiphophene **118** as model compound, and Mes*P=PMes*(**9**). A structural optimization of **9** and **113** at the B3LYP/6-31G(d) level of theory was able to reproduce the crystallographically obtained structures, albeit with slightly deviated dihedral angles. For comparison, **118** was calculated as a model compound. Since the optimized structure of **9** was similar to the crystal structure with C(*ortho*)–C(*ipso*)–P–P dihedral angle of 63° with C_2 symmetry, the structure is named as **9**(63_C_2). According to the optimized structures of **9**(63_C_2) and **113**(85_C_i), three different structures of a model compound, PhP=PPh (**118**), were optimized with fixed dihedral angle of C(*ortho*)–C(*ipso*)–P–P as 63° (two Ph rings are in C_2 symmetrical structure with C_2 axis dividing P=P double bond), 63° (two Ph rings are parallel and in $\underline{C_i}$ symmetrical structure), and 85° (two Ph rings are parallel and in C_i symmetrical structure), in which three obtained structures are denoted as **118**(85_C_i) **118**(85_C_2), and **118**(63_C_2) (Figure 10). These calculations revealed that the presence of boryl substituent in **113** raises the energy levels of all P=P-related orbitals (n, π, π*) relative to those of **118**. In contrast, all of energy levels of **113**(85_C_i) were slightly lower than those of **9**(63_C_2). From these results, the author concludes the following trend: 1) diboryldiphosphene **113** has higher P=P related orbitals due to the σ-donating effect of boryl substituent, 2) Mes*-substituted diphosphene **9** has further higher P=P related orbitals due to the introduction of three electron-donating methyl groups on the phenyl ring in comparison with phenyl-substituted diphosphene **118** regardless to the dihedral angles of **118**.

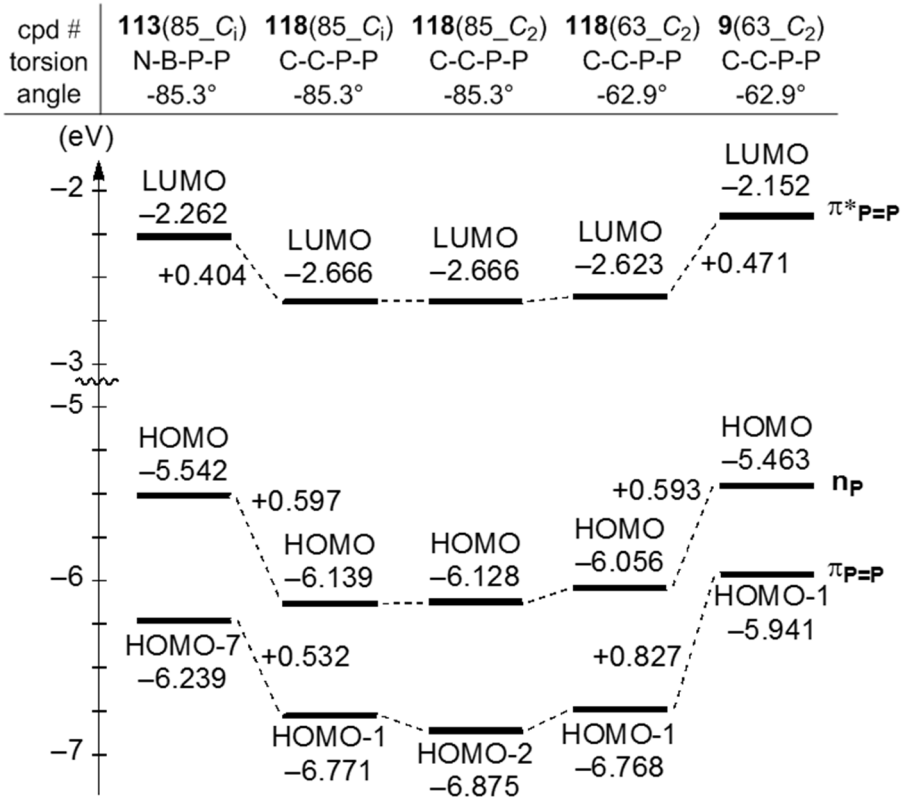

Figure 10. Calculated energy levels of $\pi^*_{P=P}$, nonbonding, and $\pi_{P=P}$ orbitals in boryl- (**113**), phenyl- (**118**), supermesityl- (**9**) substituted diphosphenes (the number in parentheses shows torsion angle between substituents and P=P planes, C_i and C_2 denotes relationship between two substituents)

2.2.6, The reaction of diboryldiphosphene with *n*butyllithium and decomposition of Mes*(*n*Bu)P-PLi(Mes*)

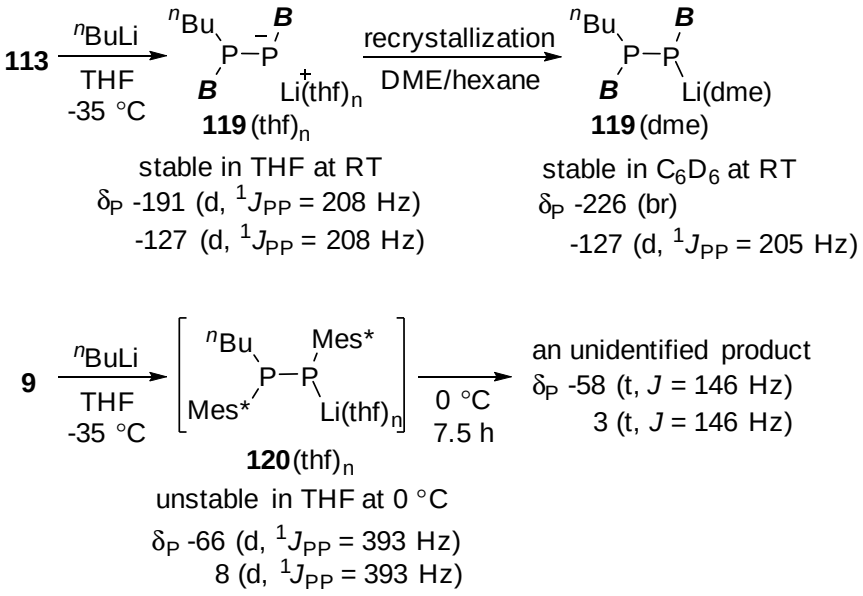

Scheme 3. Addition of *n*BuLi to diphosphenes **113** and **9**

Addition of *n*BuLi to diboryldiphosphene **113** at -35 ºC in THF afforded the stable adduct **119**(thf)$_n$, which exhibited two doublets at δ_P -192 (P-Li) and δ_P -127 (P-*n*Bu) ppm in the ^{31}P NMR spectrum (Scheme 3). The relatively large coupling constant ($^1J_{PP}$=208 Hz) is indicative of direct bonding between two inequivalent phosphorus nuclei. Considering that the ^{11}B and ^{7}Li NMR spectra of **119**(thf)$_n$ showed two distinct broad signals and one sharp singlet signal, respectively. The Li cation should be dissociated from the phosphide center to form a solvent-separated ion pair in THF, this species was found to be stable at room temperature for 9.5 h. (Figures 11, 12, and 13).

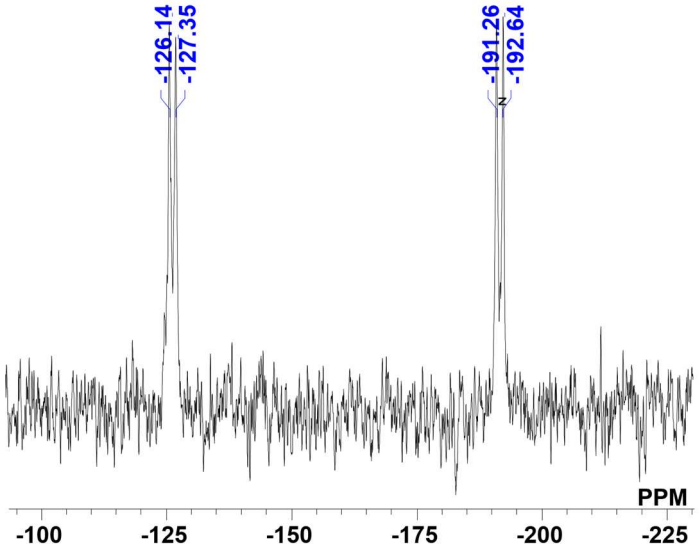

Figure 11. ^{31}P NMR spectrum of **119**(thf)$_n$.

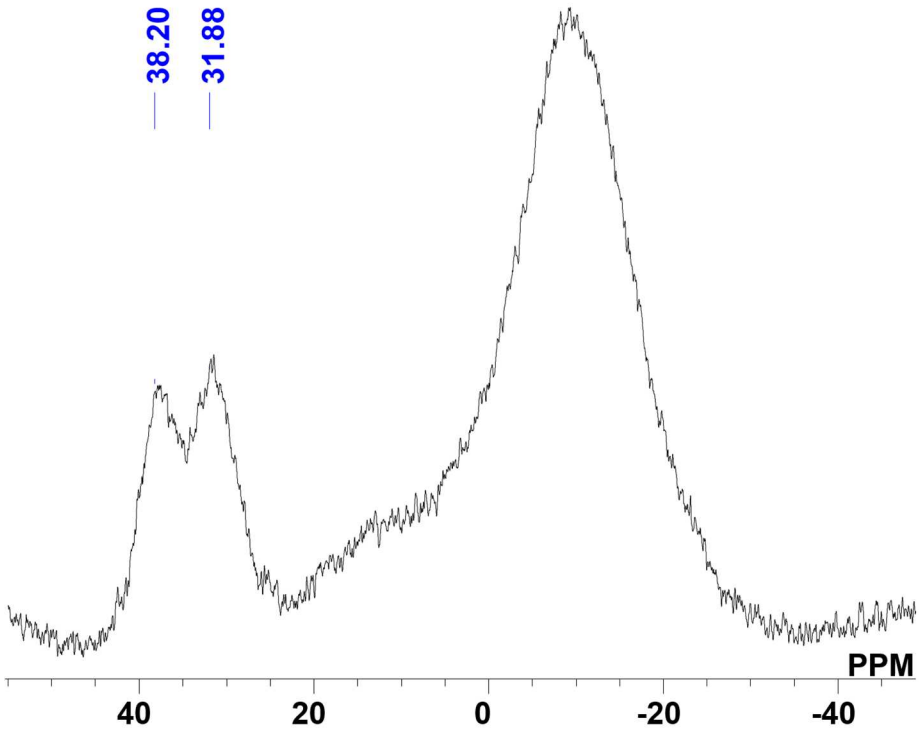

Figure 12. ^{11}B NMR spectrum of **119**$(thf)_n$.

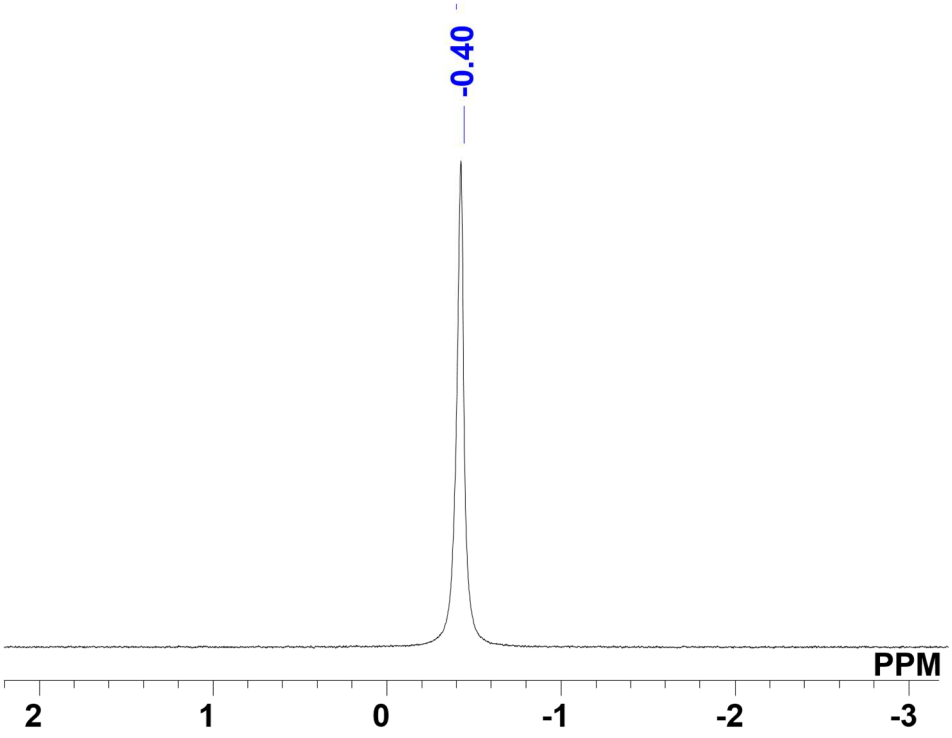

Figure 13. ^{7}Li NMR spectrum of **119**$(thf)_n$.

In contrast, treatment of **9** with ^{n}BuLi at -35 ºC in THF led the appearance of two doublet signals at δ_p -66 and δ_P 8 ppm, indicating the formation of ^{n}BuLi adduct **120**$(thf)_n$.[19] However, this species gradually decomposed at 0 ºC over the course of 7 h to generate unidentified product exhibiting two triplets at δ_P -58 and δ_P 3 ppm in the

^{31}P NMR spectrum (Figure 14). Since the related cyclotetraphosphane have also been confirmed as two triplet signals in ^{31}P NMR spectrum,[20] unidentified product may be cyclotetraphosphane **121**, which generated from dimerization of ^{n}BuP=PMes* (Scheme **4**).

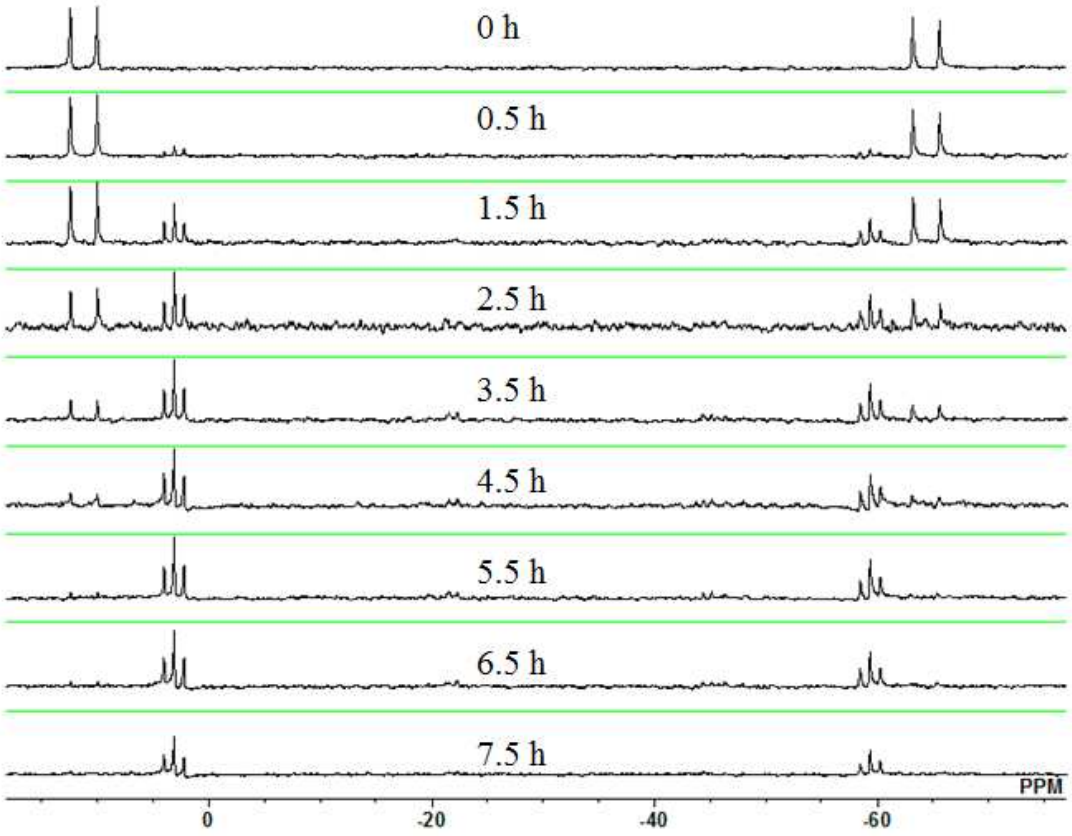

Figure 14. Time course (0-7.5 h) for the decomposition of **120**(thf)$_n$ at 0 °C

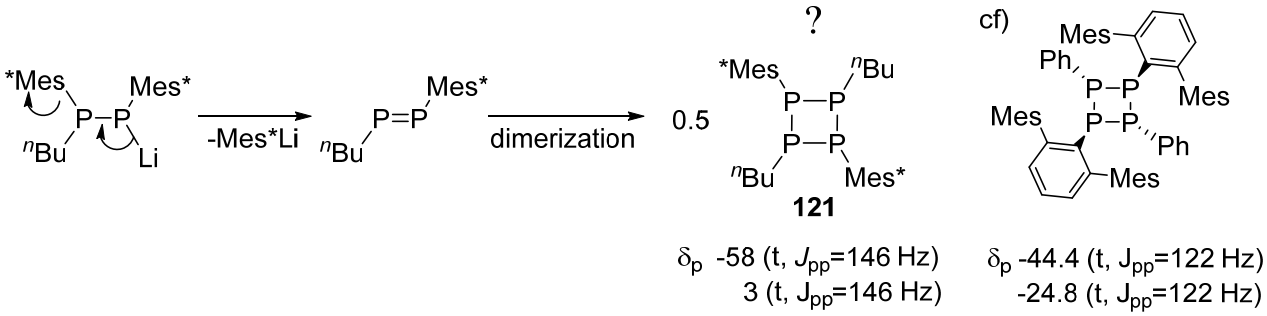

Scheme 4. Proposed mechanism of generation of cyclotetraphosphane **121**

The extraordinary stability of **119**(thf)$_n$ relative to **120**(thf)$_n$ should most likely be attributed to the presence of pπ–pπ interactions between the boryl substituent and the phosphide unit in **119**(thf)$_n$. Although the isolation of **119**(thf)$_n$ was not successful, recrystallization of **119**(thf)$_n$ from hexane in the presence of 1 equiv of DME furnished **119**(dme) as a crystalline solid. The ^{31}P NMR spectrum of **119**(dme) in C_6D_6 exhibited one doublet

signal at δ_P –116 ppm (P-^{n}Bu, $^1J_{PP}$=205 Hz) and one broad multiplet signal at δ_P -226 ppm (Figure 15). Moreover, the author confirmed ^{n}Bu group of **119**(dme) by using 1D DPFGSE-TOCSY NMR (Figure 16).

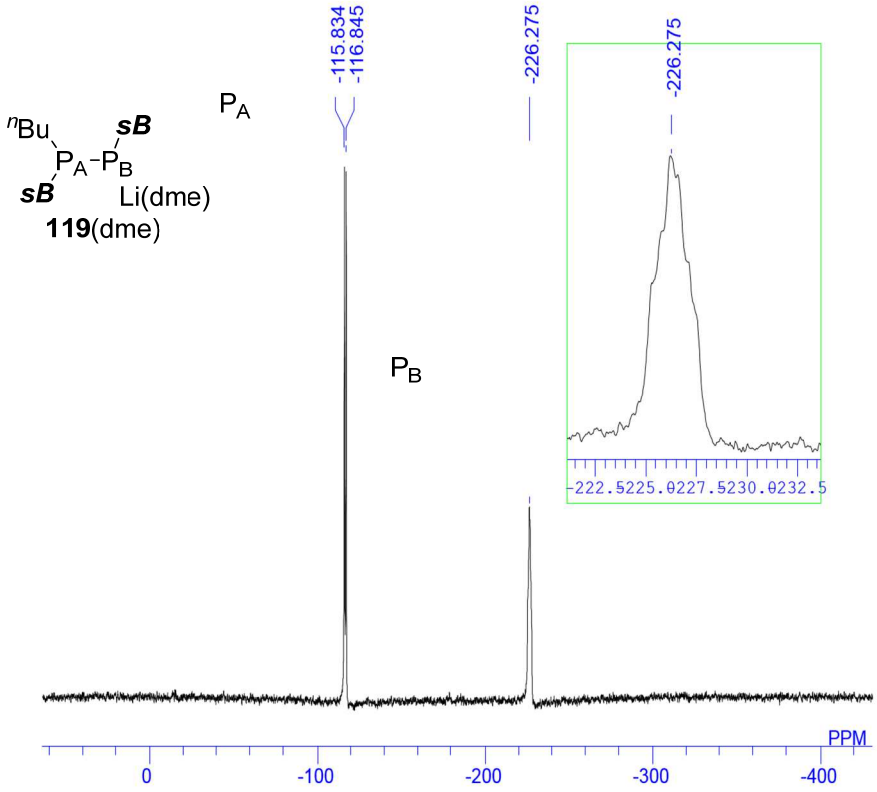

Figure 15. ^{31}P NMR spectrum of **119**(dme). The broad multiplet NMR signals at δ_p–226 ppm in phosphide moiety is probably due to the coupling with ^{31}P, ^{6}Li, and ^{7}Li.

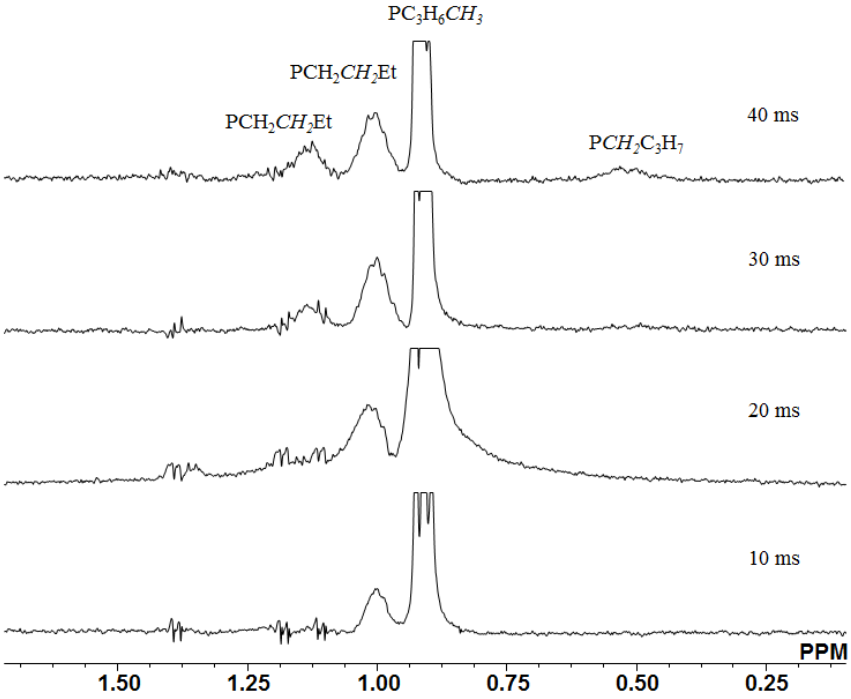

Figure 16. The 1D DPFGSE-TOCSY spectra of ^{n}Bu moiety of **119**(dme) with selective irradiation to the

terminal CH_3 with varied mixing time. With shortening the mixing time, signals disappeared in the order of the distance from the terminal CH_3.

For **119**(dme), only one very broad ^{11}B NMR signal was observed at δ_B 34 ppm, while the ^{7}Li NMR signal in C_6D_6 exhibited a doublet of doublet at δ_{Li} -4.43 ppm (Figure 17). The observed coupling constants of $^{1}J_{PLi}$=82 Hz and $^{2}J_{PLi}$=3 Hz should be attributed to interactions between lithium and the two inequivalent phosphorus nuclei (Figure 18). In their entirety, the results of this multinuclear NMR analysis indicates that **119**(dme) exists in C_6D_6 as a contact ion pair with P-Li bond in C_6D_6 solution.

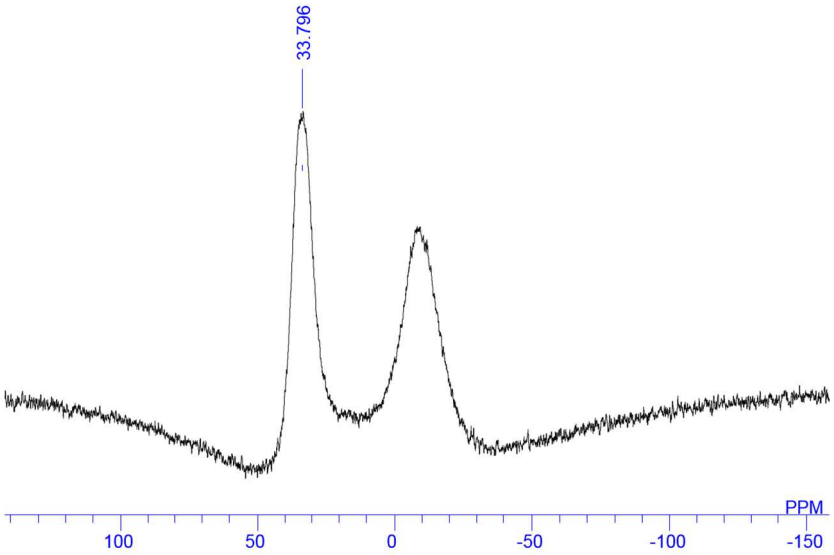

Figure 17. ^{11}B NMR spectrum of **119**(dme). The NMR signal at δ_B = 34 ppm (fwhm = 1350 Hz) is probably due to the overlapping of the two broad signals of the two inequivalent boron atoms.

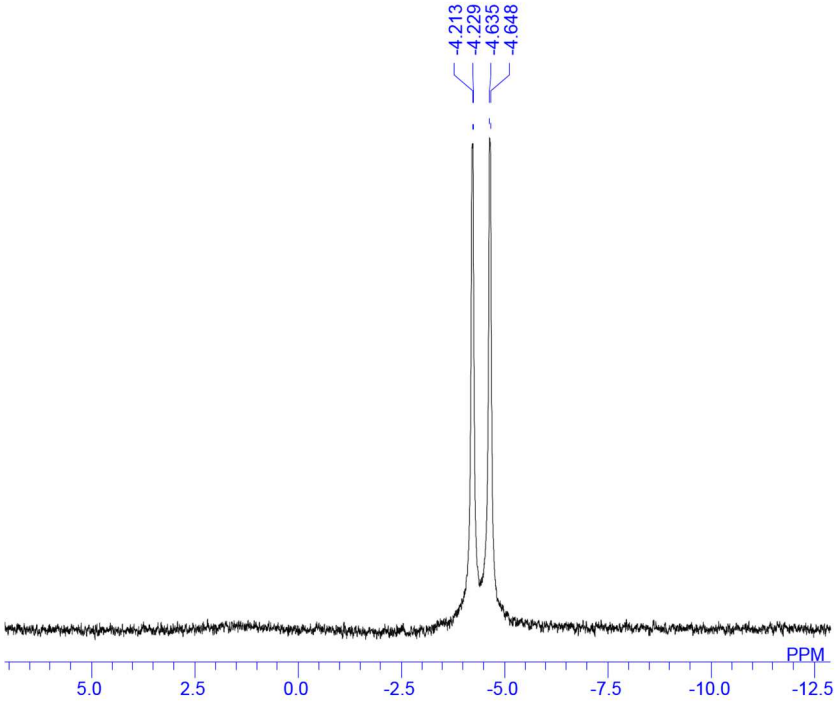

Figure 18. ^{7}Li NMR spectrum of **119**(dme).

2.2.7, X-ray structure of 119(dme)

A single-crystal X-ray diffraction analysis of **119**(dme) suggested strong pπ-pπ interactions between the anionic phosphorus atom and the adjacent boron atom (Figure 19). Single crystals of **119**(dme) contained two independent molecules of **119**(dme) and one molecule of hexane per unit cell. The two independent molecules differ with respect to each other with regard to the orientation of the diazaborole ring connected to the P2 atom. In **119**(dme), the P-B bond lengths within the phosphide moiety [1.896(3)/1.898(3) Å] were slightly shorter than those in the ^{n}Bu-substituted phosphinyl moiety in **119**(dme) [1.933(3)/1.954(3) Å]. The sum of bond angle around the phosphorus atoms (P1: 341.3°/335.5°, P2: 322.1°/312.7°) demonstrate that the pyramidalization of P1 was less pronounced than that of P2. These structural features indicate the existence of pπ-pπ interactions between P1 and the boron atom, probably due to the existence of two lone pairs on P1, and reveal that **119**(dme) exists as contact ion pair in the crystalline state.

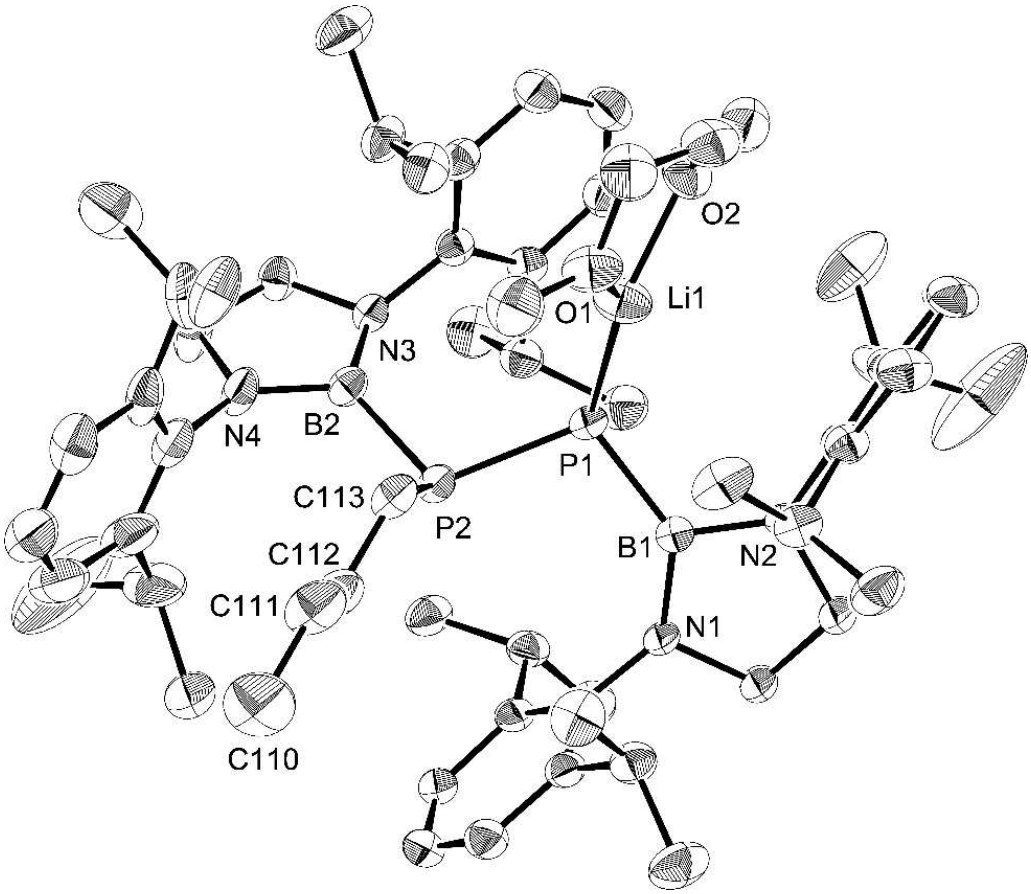

Figure 19. Molecular structure of **119**(dme) (thermal ellipsoids set at 50% probability, hydrogen atoms omitted for clarity). Selected bond lengths [Å] and angles [°]: N1-B1 1.448 (4), N2-B1 1.457 (4), P1-B1 1.896 (3), N1-B1-N2 105.2(17) N3-B2 1.445 (4), N4-B2 1.434 (4), P2-B2 1.933 (3), P1-P2 2.1775 (11)

2.2.8, DFT calculations of 119(dme)

The presence of strong pπ-pπ interactions between the anionic phosphorus atom and the adjacent boron atom in **119**(dme) was also corroborated by DFT calculations. The structural optimization of the two independent

structures encountered in the unit cells afforded two energetically similar structures, and an imaginary frequency was not found. The author selected the HOMO and the HOMO-1 of **119**(dme) correspond to the P=B π-bond and a lone pair on the phosphorus atoms, respectively (Figure 20). An NBO analysis of the resulting two structures, which described as molecules A and B in Table 1, provided estimated second-order perturbation energies of 46.78 and 54.67 kcal/mol. This result has suggested the existence of donor-acceptor interactions between the phosphorus atom of phosphide moiety and the attached boron atom. While the both molecules of A and B have showed small interactions between phosphorus atom of phosphinyl moiety and boron atom. These interactions may very likely be the key factor for the stabilization of boryl-substituted phosphinophosphide **119**(dme).

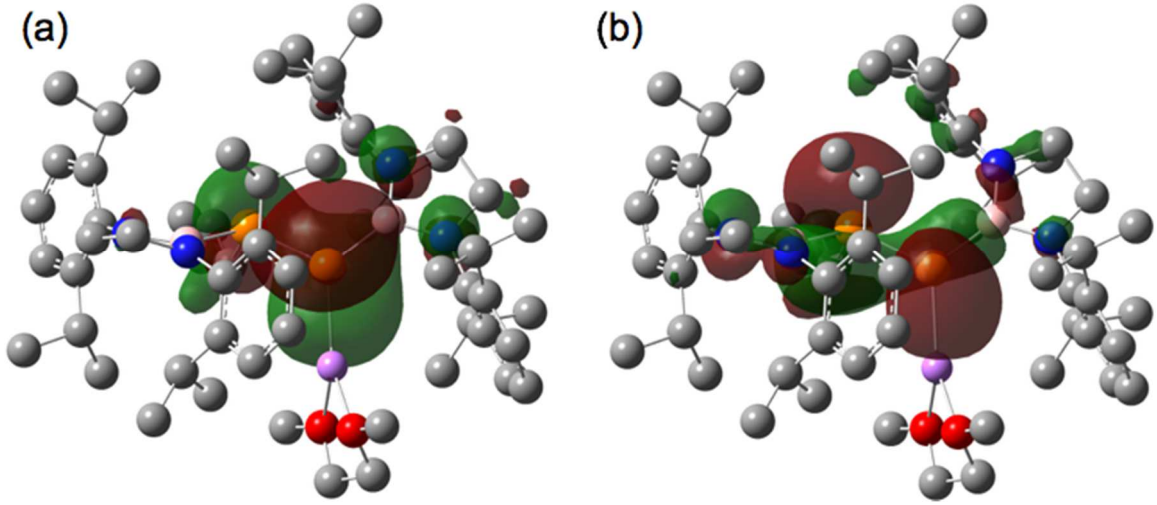

Figure 20. (a) HOMO and (b) HOMO-1 of **119**(dme) (only one of the two energetically similar structures is shown; hydrogen atoms are omitted for clarity; color code: gray = carbon, blue = nitrogen, orange = phosphorus, pale pink = boron, purple = lithium, red = oxygen).

Table 2. Donor-acceptor interaction (kcal/mol) in **119**(dme) estimated by the second order perturbation theory analysis.

molecule	atom	N to B	P to B
A	P coordinating to Li	55.40 55.96	46.78
	^{n}Bu-substituted P	67.02 59.28	0.57
B	P coordinating to Li	55.32 53.79	54.67
	^{n}Bu-substituted P	57.83 61.56	18.40

2.3. Conclusion

Boryl-substituted diphosphene **113** was synthesized by a nucleophilic borylation of PCl_3 using a borylzinc reagent. A single-crystal X-ray diffraction analysis in combination with DFT calculations and an analysis of UV/Vis spectroscopic results revealed a σ-donating effect of boryl substituents in **113** that is slightly weaker than that of the Mes* substituent. The reaction of **113** with ^{n}BuLi resulted in the formation of a phosphinophosphide that was stabilized by a π-accepting effect of boryl substituent, which was confirmed by single-crystal X-ray diffraction analysis and DFT calculations.

Experimental procedure

General

All manipulations involving the air- and moisture-sensitive compounds were carried out in a glovebox (Miwa MFG and Korea KIYON) under argon. Ether, THF, toluene, and *n*-hexane were purified by passing through a solvent purification system (Grass Contour). Lithium dispersion (purchased from Kanto Chemical Co., Inc., containing 1% sodium) was washed with hexane before the use to make a lithium powder. NMR spectra were recorded on 500 or 400 MHz spectrometers. Chemical shifts are reported in ppm relative to the residual partially protonated solvent for ^{1}H, deuterated solvent for ^{13}C, external $BF_3 \cdot OEt_2$ for ^{11}B and 85% H_3PO_4 for ^{31}P nuclei. Data are presented in the following space: chemical shift, multiplicity (s = singlet, d = doublet, t = triplet, sept = septet, m = multiplet, br = broad, brs = broad singlet), coupling constant in hertz (Hz), and signal area integration in natural numbers. Mass spectra were measured on a JEOL JMS-700 mass spectrometer. Melting points were determined on Optimelt (SRS) and were uncorrected. Elemental analyses were carried out at the A Rabbit Science Japan Co., Ltd. X-ray crystallographic analysis was performed on VariMax/Saturn CCD diffractometer.

Synthesis of 114

A dichloromethane solution of BCl_3 (1.0 M, 56.0 mL, 56.0 mmol) was added to a hexane solution of *N,N*-Bis(2,6-diisopropylphenyl)ethylenediamine (15.3 g, 40.0 mmol) at room temperature under argon atmosphere. After stirring the reaction mixture for 50 min at room temperature, volatiles were evaporated under reduced pressure. Then, CH_2Cl_2 (200 mL) and NEt_3 (68.9 g, 360.0 mmol, 50 mL) were subsequently added to the residue at room temperature. The resulting suspension was stirred for 15 h at 50 °C. After volatiles were evaporated under reduced pressure, hexane was added to the residue. The resulting suspension was filtered through a pad of Celite. Volatiles were removed from the filtrate to give a white solid of **114** (13.2 g, 3.11 mmol, 78 %). An analytically pure sample was obtained by recrystallization from hexane. ^{1}H NMR (C_6D_6, 500 MHz) δ 1.30 (d, *J* = 7 Hz, 12H), 1.36 (d, *J* = 7 Hz, 12H), 3.40 (s, 4H), 3.46 (sep, *J* = 7 Hz, 4H), 7.13-7.16 (m, 4H), 7.21 (dd, *J* = 7, 9 Hz, 2H); ^{13}C NMR (C_6D_6, 125 MHz) δ 24.6 (CH_3), 25.0 (CH_3), 28.9 (CH), 52.2 (CH_2), 124.2 (CH), 127.8 (CH), 138.0 (4°), 147.7 (4°); ^{11}B NMR (C_6D_6, 160 MHz) δ 24 (br s); mp: 180.6-181.1 °C. Anal. calcd. for $C_{26}H_{38}BClN_2$: C, 73.50; H, 9.02; N, 6.59. Found: C, 73.73; H, 9.00; N, 6.71.

Synthesis of (**116**·thf)$_2$

In a glovebox, a 30 mL vial equipped with a glass magnetic stirring bar was charged with **114** (2.00 g, 4.71 mmol), lithium powder (0.370 g, 47.1 mmol), and naphthalene (0.604 g, 4.71 mmol). To the mixture, in THF (15 mL) at –35 ºC for 25 h. The reaction mixture was filtered through a pad of Celite and the residue was washed with THF (10 mL). The resulting solution was added to a THF (10 mL) solution of $ZnCl_2$ (0.771 g, 5.66 mmol) at –35 °C and the resulting mixture was stirred at –35 °C for 20 min. After volatiles were removed from the reaction mixture under reduced pressure, the residue was triturated with hexane. The resulting suspension was filtered through a pad of Celite to remove inorganic salts. After solvent was removed from the filtrate under reduced pressure, the residue was recrystallized from hexane/THF to give (**116**·thf)$_2$ as colorless crystals (0.745 g, 0.668 mmol, 28%). Recrystallization of the product from CH_3CN solution gave single crystals of (**116**·$NCCH_3$)$_2$·$2CH_3CN$ suitable for X-ray analysis. ^{1}H NMR (C_6D_6, 500 MHz) δ 1.24 (br, 4H, THF), 1.28 (d, *J* = 7 Hz, 12H), 1.31 (d, *J* = 7 Hz, 12H), 3.26 (br, 4H, THF), 3.55 (s, 4H), 3.62 (sept, *J* = 7 Hz, 4H), 7.10 (d, 4H), 7.13-7.17 (m); ^{13}C NMR (C_6D_6, 125 MHz) δ 25.0 (CH_2), 25.1 (CH_3), 25.3 (CH_3), 28.5 (CH), 54.6 (CH_2), 68.4 (CH_2), 123.8 (CH), 126.6 (CH), 142.0 (4°), 148.0 (4°); ^{11}B NMR (C_6D_6, 160 MHz) δ 34 (br s); mp: 181.9-184.7 °C. Anal. calcd. for $C_{60}H_{92}B_2Cl_2N_4O_2Zn_2$: C, 64.07; H, 8.25; N, 4.98. Found: C, 63.94; H, 8.33; N, 5.11.

Synthesis of 117

In a glovebox, PCl_3 (119 μL, 1.37 mmol) was added to a CH_3CN (20 mL) solution of (**116**·thf)$_2$ (460 mg, 0.912 mmol) at room temperature. After the reaction mixture was stirred at room temperature for 9 h, volatiles were removed under reduced pressure. The residue was triturated with hexane and the resulting suspension was filtered through a pad of Celite to remove inorganic salts. After volatiles were removed from the filtrate under reduced pressure, the residue was recrystallized from hexane to give a pale yellow solid of **117** (251 mg, 56%). ^{1}H NMR (C_6D_6, 500 MHz) δ 1.24 (d, *J* = 7 Hz, 12H), 1.34 (d, *J*= 7 Hz, 12H), 3.53 (s, 4H), 3.61 (sept, *J* = 7 Hz, 4H), 7.09 (d, *J* = 8 Hz, 4H), 7.17 (dd, *J* = 7, 8 Hz, 2H); ^{13}C NMR ($CDCl_3$, 125 MHz) δ 24.1 (CH_3), 26.1 (CH_3), 28.6 (CH), 54.4 (CH_2), 124.0 (CH), 127.4 (CH), 138.0 (4°), 147.2 (4°); ^{11}B NMR ($CDCl_3$, 160 MHz) δ 26 (br s); ^{31}P NMR ($CDCl_3$, 160 MHz) δ 158 (s); mp: 98.9-182.3 ºC. (decomp); Anal. calcd. for $C_{26}H_{38}BCl_2N_2P$: C, 63.56; H, 7.80; N, 5.70. Found: C, 63.68; H, 8.05; N, 5.66.

Synthesis of 113

In a glovebox, a solution of **117** (0.251 g, 0.511 mmol) in THF (3.00 mL) was added to magnesium (13.6 mg, 0.562 mmol) in a 3 mL vial at –35 °C in refrigerator of glovebox. The resulting mixture was stirred for 34 h at –35 °C, during which time the color of the solution changed from colorless to red. After the reaction mixture was evaporated under reduced pressure, the residue was triturated with toluene (50 mL). The resulting suspension was filtered to remove $MgCl_2$ through a pad of Celite. Volatiles were evaporated from the filtrate under reduced pressure. The resulting green solid residue was filtered through a glass filter and was washed with Et_2O to give **113** as a yellow solid (102 mg, 47%). ^{1}H NMR (C_6D_6, 500 MHz) δ 0.97 (d, *J* = 7 Hz, 12H), 1.23 (d, *J* = 7 Hz, 12H), 3.56 (s, 4H), 3.63 (sept, *J* = 7 Hz, 4H), 6.98 (d, *J* = 8 Hz, 8H), 7.12 (t, *J* = 7 Hz, 4H); ^{13}C NMR (C_6D_6, 125 MHz) δ 24.5 (CH_3), 26.0 (CH_3), 28.5 (CH), 54.3 (CH_2), 124.0 (CH), 127.1 (CH), 139.6 (4°), 147.3 (4°); ^{11}B NMR (C_6D_6, 160 MHz) δ 32 (br s); ^{31}P NMR (C_6D_6, 160 MHz) δ 605 (s): mp: 212.7-

217.1 °C. Anal. calcd. for $C_{52}H_{76}B_2N_4P_2$: C, 74.29; H, 9.11; N, 6.66. Found: C, 74.17; H, 9.41; N, 6.59.

NMR observation of 119(thf)$_n$ generated by the reaction of 113 with ^{n}BuLi

In a glovebox, precooled (–35 °C) ^{n}BuLi (12.0 μL, 19.9 μmol, 1.66 M) was added to a precooled (–35 °C) solution of **113** (14.7 mg, 18.1 μmol) in THF (0.500 mL) in a 15 mL vial. After stirring the resulting solution at –35 °C for 10 min, the reaction mixture was transferred to a precooled J-Young NMR tube. The NMR tube was quickly brought out from the glovebox and NMR spectra were recorded at 0 °C. After leaving the NMR tube 9.5 h at room temperature, NMR spectra were recorded again to confirm the stability of **119**(thf)$_n$ at room temperature.

Isolation of 119(dme)

In a glovebox, a precooloed (–35 °C) THF solution (15 mL) of **113** (188 mg, 0.232 mmol) was added to a precooloed (–35 °C) *n*-BuLi solution (1.64 M, 161 μL, 0.264 mmol) in hexane. After stirring the reaction mixture for 30 min at –35 °C, the solvents were evaporated under reduced pressure. Addition of toluene (2 mL) to the reaction mixture and removal of volatiles under reduced pressure were repeated two times to remove THF completely. The reaction mixture was recrystallized from hexane solution in the presence of DME (24.1 μL, 0.232 mmol, 1 equiv. to **113**) to give **119**(dme) as colorless crystalline solids (140 mg, 0.141 mmol, 61%). ^{1}H NMR [C_6D_6, 500 MHz, 60 °C, signals of ^{n}Bu group were assigned with 1D-TOCSY spectra with selective irradiation to the terminal CH_3 in ^{n}Bu group and varied mixing time(Figure 16)] δ 0.56 (m, 2H, P*CH*$_2$CH$_2$CH$_2$CH$_3$), 0.93 (t, *J* = 7 Hz, 3H, PCH$_2$CH$_2$CH$_2$*CH*$_3$), 1.05 (m, 2H, PCH$_2$CH$_2$*CH*$_2$CH$_3$), 1.13 (m, 2H, PCH$_2$*CH*$_2$CH$_2$CH$_3$), 1.15 (d, *J* = 7 Hz, 12H), 1.22 (d, *J* = 7 Hz, 12H), 1.38 (d, *J* = 7 Hz, 12H), 1.41 (d, *J* = 7 Hz, 12H) 3.12 (s, 6H), 3.30 (s, 4H), 3.43 (s, 4H), 3.54 (s, 4H), 3.62 (sept, *J* = 7 Hz, 4H), 3.68 (sept, *J* = 7 Hz, 4H), 6.92-6.99 (m, 6H), 7.03-7.09 (m, 6H); ^{13}C NMR (C_6D_6, 125 MHz, 60 °C) δ 14.5 (s, PCH$_2$CH$_2$CH$_2$*CH*$_3$), 24.3 (CH$_3$), 24.4 (CH$_3$), 25.4 (d, *J* = 8 Hz, PCH$_2$CH$_2$*CH*$_2$CH$_3$), 26.3 (CH$_3$), 28.2 (dd, *J* = 24 Hz, 7 Hz, P*CH*$_2$CH$_2$CH$_2$CH$_3$), 28.7 (*CH*Me$_2$), 32.7 (dd, *J* = 6 Hz, 4 Hz, PCH$_2$*CH*$_2$CH$_2$CH$_3$), 53.9 (N*CH*$_2$), 54.5 (N*CH*$_2$), 58.8 (O*CH*$_3$), 72.2 (O*CH*$_2$), 123.6 (CH), 124.0 (CH), 126.0 (CH), 126.2 (CH), 143.4 (4°), 144.7(4°), 149.11 (4°), 149.15 (4·); ^{11}B NMR (THF-d_8, 160 MHz) 34 (br, half width ~ 1350 Hz, probably due to overlapping two broad signals of two inequivalent boron atoms); ^{31}P NMR (C_6D_6, 160 MHz) δ –116 (d, *J* = 205 Hz), –226 (brm, probably due to the coupling with ^{31}P, ^{6}Li, and ^{7}Li); ^{7}Li NMR (C_6D_6, 194 MHz) –4.43 (dd, *J* = 82, 3 Hz); mp: 186.2-204.7 ºC (decomp); HRMS (ESI$^+$) *m/z* Calcd. for $C_{56}H_{87}B_2N_4P_2$ [M+H–Li–DME]$^+$: 899.6592, found: 899.6588.

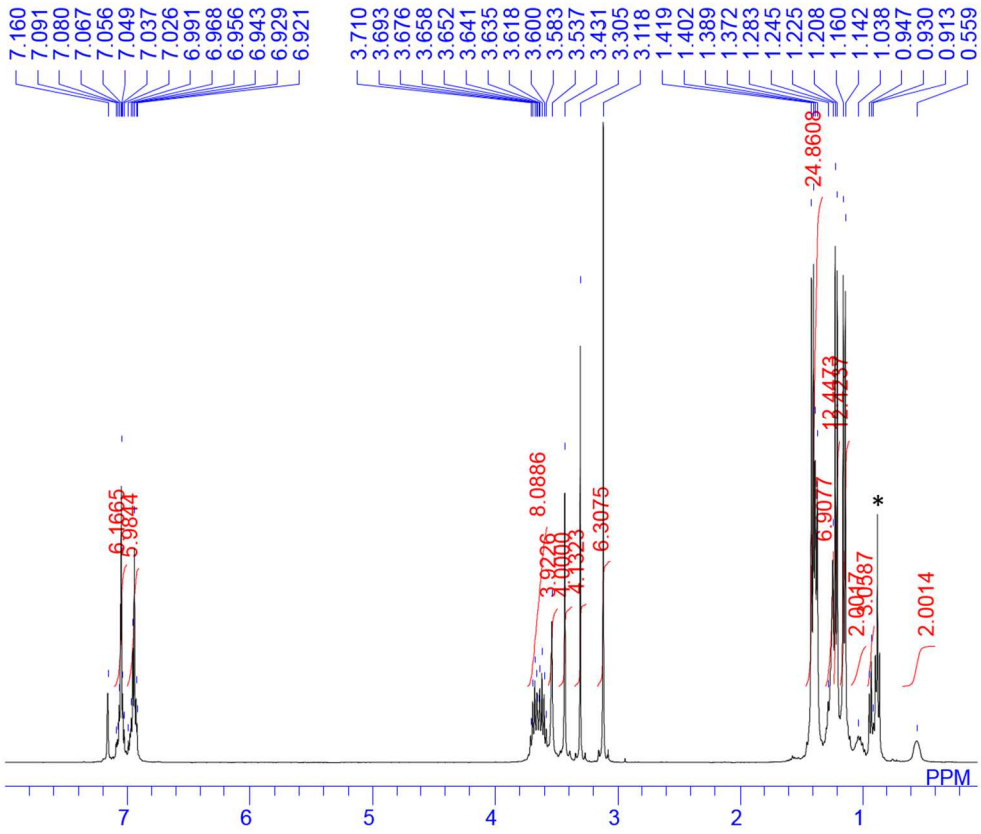

Figure S1. [1]H NMR spectrum of **119**(dme) (* denotes signal of *n*-hexane)

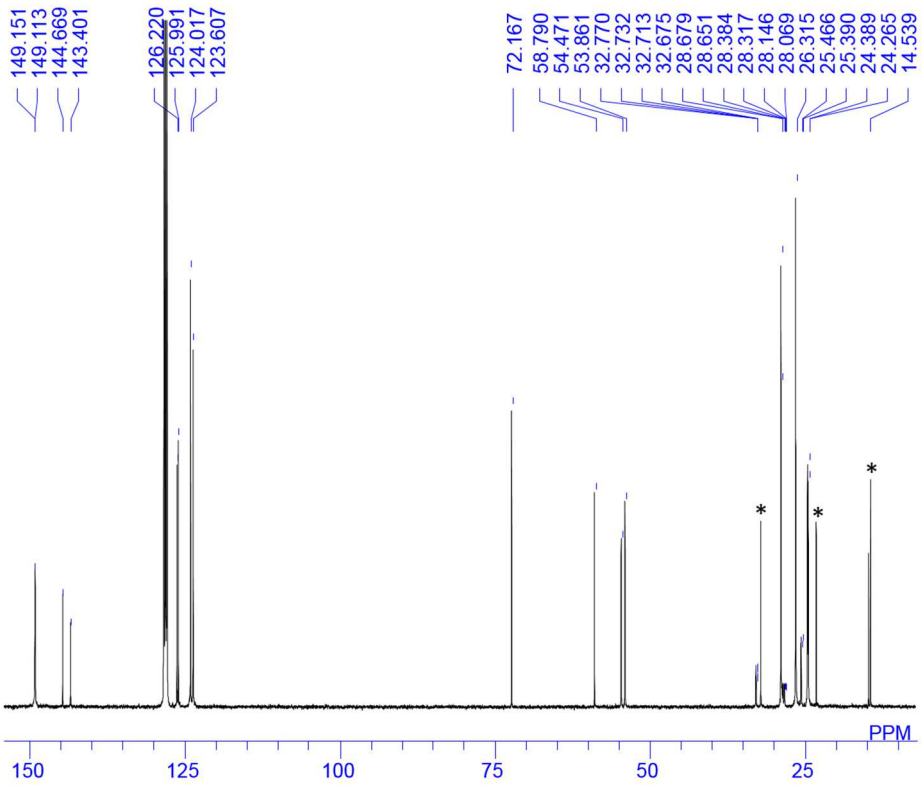

Figure S2. [13]C NMR spectrum of **119**(dme) (* denotes signals of *n*-hexane)

NMR measurement at 0 °C to monitor the decomposition of 120(thf)$_n$ generated by the reaction of 1 with ^{n}BuLi at –35 °C

In a glovebox, precooled (–35 °C) ^{n}BuLi (20.9 μL, 54.3 μmol, 1.64 M) was added to a precooled (–35 °C) solution of **9** (20.0 mg, 36.2 μmol) in THF (1.0 mL) in a 3 mL vial. The resulting solution was transferred to a precooled (–35 °C) NMR tube. The NMR tube was quickly brought out from the glovebox and was loaded to a precooled NMR probe at -30 ºC. After elevating temperature of the probe to 0 °C, NMR spectra were repeatedly recorded at 0 °C (Figure 14). The resulting two triplet signals could not be completely characterized.

2. Details for X-Ray Crystallography

Details of the crystal data and a summary of the intensity data collection parameters for **113**, **114**, (**116**·$NCCH_3$)$_2$·$2CH_3CN$, (**116**·thf)$_2$·CH_2Cl_2, **117**, and **119**(dme) are listed in Table S1. ORTEP drawings of the compounds, which are not displayed in main text, are illustrated as Figures S3-S5. In each case a suitable crystal was mounted with a mineral oil to the glass fiber and transferred to the goniometer of a Rigaku Mercury CCD or a VariMax Saturn CCD diffractometer with graphite-monochromated Mo Kα radiation (λ = 0.71075 Å). All the following procedure for analysis, Yadokari-XG 2009[21] was used as a graphical interface. The structures were solved by direct method with (SIR-2014 and SIR-97)[22] and refined by full-matrix least-squares techniques against F^2 (SHELXL-2014).[23] The intensities were corrected for Lorentz and polarization effects or NUMABS program (Rigaku 2005). The non-hydrogen atoms were refined anisotropically. Hydrogen atoms were placed using AFIX instructions. Because of the hard disorder of CH_2Cl_2 molecule in (**116**·thf)$_2$·CH_2Cl_2, SQUEEZE by PLATON[24] was applied. All the resulting CIF files were deposited to Cambridge Crystallographic Data Center.

Table S1. Crystallographic data and structure refinement details for **113**, **114**, (**116**·$NCCH_3$)$_2$·$2CH_3CN$, (**116**·thf)$_2$·CH_2Cl_2, **117**, and **119**(dme).

	113	**114**	(**116**·$NCCH_3$)$_2$·$2CH_3CN$	(**116**·thf)$_2$·CH_2Cl_2	**117**	**119**(dme)
CCDC deposit #	1491008	1491009	1491010	1491011	1491012	1491013
Empirical formula	$C_{52}H_{76}B_2N_4P_2$	$C_{26}H_{38}BClN_2$	$C_{60}H_{88}B_2Cl_2N_8Zn_2$	$C_{121}H_{186}B_4Cl_6N_8O_4Zn_4$	$C_{26}H_{38}BCl_2N_2P$	$C_{132}H_{218}B_4Li_2N_8O_4P_4$
Formula weight	840.72	424.84	1144.64	2334.19	491.26	2162.13
T (K)	93(2)	93(2)	93(2)	93(2)	113(2)	93(2)
Crystal system	*Monoclinic*	*Monoclinic*	*Monoclinic*	*Tetragonal*	*Monoclinic*	*Triclinic*
Space group	$P2_1/n$	$P2_1/n$	$P2_1/n$	$I4_1/a$	$P2_1/n$	P-1
a (Å)	13.084(6)	19.271(3)	13.317(3)	29.607(6)	9.395(2)	12.3796(16)
b (Å)	14.600(6)	6.7904(11)	14.422(3)	29.607(6)	14.493(3)	21.551(3)
c (Å)	14.667(7)	19.475(3)	16.548(3)	14.542(3)	20.225(5)	25.488(3)
α (°)	90	90	90	90	90	100.147(3)
β (°)	113.916(6)	105.294(2)	102.056(3)	90	99.851(4)	97.501(2)
γ (°)	90	90	90	90	90	96.4438(17)
V (Å^3)	2561(2)	2458.1(7)	3108.0(10)	12747(5)	2713.3(11)	6572.6(15)

Z	2	4	2	4	4	2
$D_{calc,}$ (g/m^3)	1.090	1.148	1.223	1.216	1.203	1093
μ (mm^{-1})	0.122	0.170	0.900	0.920	0.315	0.110
F(000)	912	920	1216	4968	1048	2368
Crystal size (mm)	0.07×0.07×0.03	0.40×0.18×0.16	0.09×0.08×0.07	0.20×0.15×0.05	0.40×0.30×0.15	0.36×0.22×0.18
2θ range (°)	1.763-31.463	3.465-27.482	3.022-27.478	3.077-27.461	2.044-27.558	3.005-27.453
reflns collected	24470	19186	25193	51473	20680	54015
Indep. reflns/R_{int}	7683/0.0927	5618/0.0356	7108/0.0615	7224/0.0547	6201/0.0390	28901/0.0416
param	317	279	344	333	335	1438
GOF on F^2	1.041	1.141	1.075	1.102	1.099	1.067
R_1, wR_2 [I>2σ(I)]	0.0799, 0.1716	0.0533, 0.1260	0.0544, 0.1101	0.0455, 0.1078	0.0483, 0.1000	0.0851, 0.2067
R_1, wR_2 (all data)	0.1537, 0.2137	0.0612, 0.1326	0.0749, 0.1217	0.0520, 0.1118	0.0662, 0.1085	0.1201, 0.2378

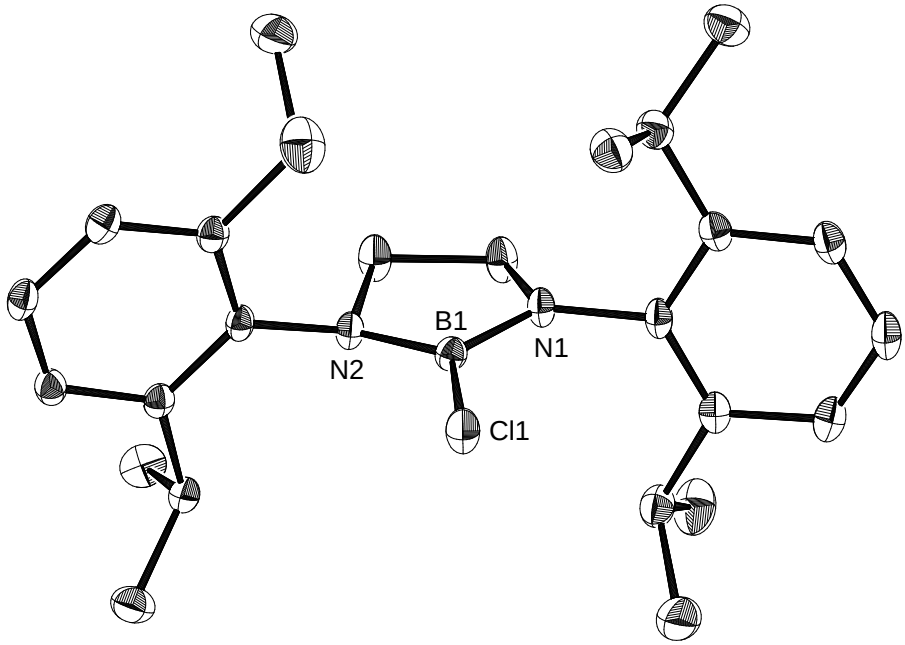

Figure S3. Molecular structure of **114** (thermal ellipsoids set at 50% probability, hydrogen atoms are omitted for clarity)

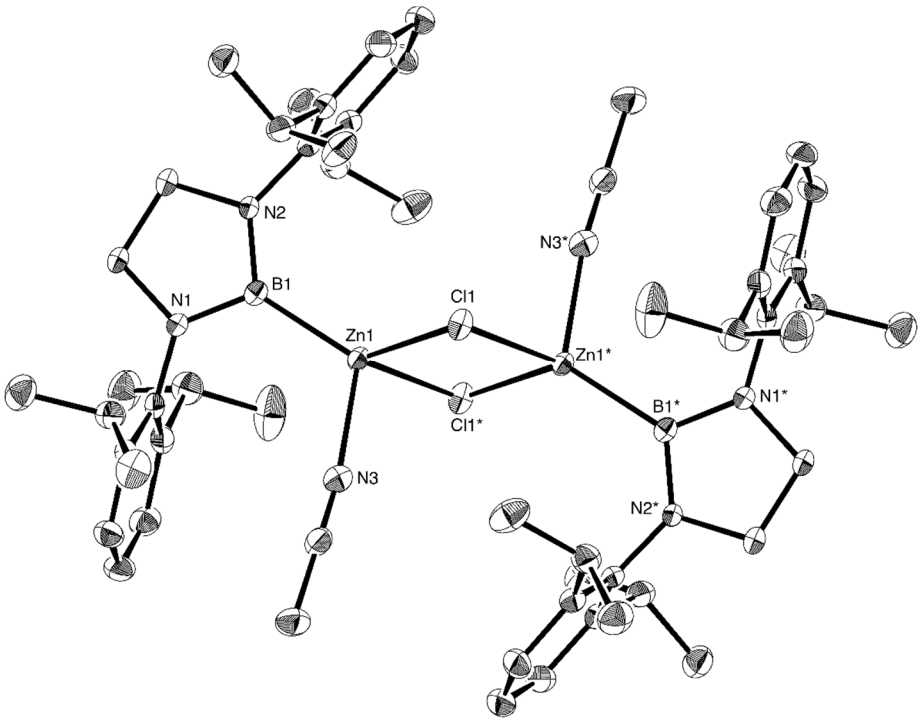

Figure S4. Molecular structure of (**116**·$NCCH_3$)$_2$·CH_3CN (thermal ellipsoids set at 50% probability, hydrogen atoms and co-crystallized CH_3CN molecule are omitted for clarity, asterisks denote atoms generated by symmetry operation)

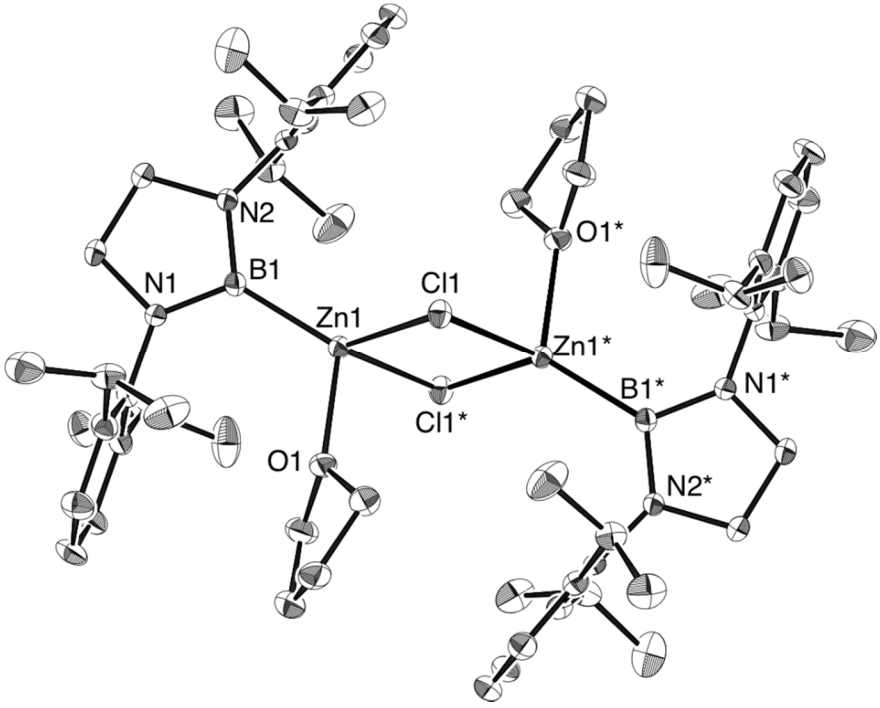

Figure S5. Molecular structure of (**116**·thf)$_2$·CH_2Cl_2 [thermal ellipsoids set at 50% probability, hydrogen atoms and co-crystallized CH_2Cl_2 molecule (SQUEEZED) are omitted for clarity, asterisks denote atoms generated by symmetry operation]

Reference

(1) Boron-Containing Polymers, Doshi, A. Jäkle, F. in *Comprehensive Inorganic Chemistry II (Second Edition)* (Ed.: J. R. Poeppelmeier), Elsevier, Amsterdam, **2013**, pp. 861-891; (b) Rao,Y.-L.; Amarne, H.; Wang, S. *Coord. Chem. Rev.* **2012**, *256*, 759. (c) Jäkle, F. *Chem. Rev.* **2010**, *110*, 3985; (d) Swamy, C. A.; Priyanka, R. N.; Thilagar, P. *Dalton Trans.* **2014**, *43*, 4067. (e) Yin, X.; Chen, J.; Lalancette, R. A.; Marder, T. B.; Jäkle, F. *Angew. Chem. Int. Ed.* **2014**, *53*, 9761. (f) Ji, L.; Edkins, R. M.; Sewell, L. J.; Beeby, A.; Batsanov, A. S.; Fucke, K.; Drafz, M.; Howard, J. A. K.; Moutounet, O.; Ibersiene, F.; Boucekkine, A.; Furet, E.; Liu, Z.; Halet, J.-F.; Katan, C.; Marder, T. B. *Chem. Eur. J.* **2014**, *20*, 13618. (g) Braunschweig, H.; Dyakonov, V.; Engels, B.; Falk, Z.; Hörl, C.; Klein, J. H.; Kramer, T.; Kraus, H.; Krummenacher, I.; Lambert, C.; Walter, C. *Angew. Chem. Int. Ed.* **2013**, *52*, 12852. (h) Weber, L.; Eickhoff, D.; Marder, T. B.; Fox, M. A.; Low, P. J.; Dwyer, A. D.; Tozer, D. J.; Schwedler, S.; Brockhinke, A.; Stammler, H.-G.; Neumann, B. *Chem. Eur. J.* **2012**, *18*, 1369. (i) Weber, L.; Halama, J.; Böhling, L.; Chrostowska, A.; Dargelos, A.; Stammler, H.-G.; Neumann, B. *Eur. J. Inorg. Chem.* **2011**, *2011*, 3091. (j) Chen, P.; Lalancette, R. A.; Jäkle, F. *J. Am. Chem. Soc.* **2011**, *133*, 8802. (k) Weber, L.; Werner, V.; Fox, M. A.; Marder, T. B.; Schwedler, S.; Brockhinke, A.; Stammler, H.-G.; Neumann, B. *Dalton Trans.* **2009**, 1339. (l) Entwistle, C. D.; Collings, J. C.; Steffen, A.; Palsson, L.-O.; Beeby, A.; Albesa-Jove, D.; Burke, J. M.; Batsanov, A. S.; Howard, J. A. K.; Mosely, J. A.; Poon, S.-Y.; Wong, W.-Y.; Ibersiene, F.; Fathallah, S.; Boucekkine, A.; Halet, J.-F.; Marder, T. B. *J. Mater. Chem.* **2009**, *19*, 7532.

(2) (a) Protchenko, A. V.; Birjkumar, K. H.; Dange, D.; Schwarz, A. D.; Vidovic, D.; Jones, C.; Kaltsoyannis, N.; Mountford, P.; Aldridge, S. *J. Am. Chem. Soc.* **2012**, *134*, 6500. (b) Protchenko, A. V.; Dange, D.; Harmer, J. R.; Tang, C. Y.; Schwarz, A. D.; Kelly, M. J.; Phillips, N.; Tirfoin, R.; Birjkumar, K. H.; Jones, C.; Kaltsoyannis, N.; Mountford, P.; Aldridge, S. *Nat. Chem.* **2014**, *6*, 315.

(3) (a) Yoshifuji, M.; Shima, I.; Inamoto, N.; Hirotsu, K.; Higuchi, T. *J. Am. Chem. Soc.* **1981**, *103*, 4587; (b) Yoshifuji, M.; Shima, I.; Inamoto, N.; Hirotsu, K.; Higuchi, T. *J. Am. Chem. Soc.* **1982**, *104*, 6167; (c) Weber, L. *Chem. Rev.* **1992**, *92*, 1839. (d) Baumgartner, T.; Réau, R. *Chem. Rev.* **2006**, *106*, 4681.

(4) Cowley, A.; H. Kilduff, J. E.; Newman, T. H.; Pakulski, M. *J. Am. Chem. Soc.* **1982**, *104*, 5820.

(5) (a) Cowley, A. H.; Knueppel, P. C.; Nunn, C. M. *Organometallics* **1989**, *8*, 2490. (b) Weber, L.; Meine, G.; Boese, R.; Augart, N. *Organometallics* **1987**, *6*, 2484. (c) Wiberg, N.; Wörner, A.; Lerner, H.-W.; Karaghiosoff, K. *Z. Naturforsch., B: Chem. Sci.* **2002**, *57*, 1027; (d) Cappello, V.; Baumgartner, J.; Dransfeld, A.; Flock, M.; Hassler, K. *Eur. J. Inorg. Chem.* **2006**, 2393.

(6) Markovskii, L. N.; Romanenko, V. D.; Povolotskii, M. I.; Ruban, A. V.; Klebanskii, E. O. *Zh. Obshch. Khim.* **1986**, *56*, 2157.

(7) (a) Niecke, E.; Rüger, R.; Lysek, M.; Pohl, S.; Schoeller, W. *Angew. Chem. Int. Ed. Engl.* **1983,** *22*, 486; (b) Niecke, E.; Rüger, R. *Angew. Chem. Int. Ed. Engl.* **1983,** *22*, 155.

(8) (a) Usharani, D.; Poduska, A.; Nixon, J. F.; Jemmis, E. D. *Chem. Eur. J.* **2009**, *15*, 8429 (b) Vogt-Geisse, S.; Schaefer, H. F. *J. Chem. Theory Comput.* **2012,** *8*, 1663.

(9) Fischer, R. C.; Power, P. P. *Chem. Rev.* **2010,** *110*, 3877.

(10) Graduation thesis of Masafumi Okamoto

(11) (a) Kajiwara, T.; Terabayashi, T.; Yamashita, M.; Nozaki, K. *Angew. Chem. Int. Ed.* **2008**, *47*, 6606. (b)

Campos, J.; Aldridge, S. *Angew. Chem. Int. Ed.* **2015**, *54*, 14159.
(12) Dange, D.; Davey, A.; Abdalla, J. A. B.; Aldridge, S.; Jones, C. *Chem. Commun.* **2015**, *51*, 7128.
(13) Emsley, J. *The Elements*, 3rd ed., Oxford University Press, New York, **1998**.
(14) (a) Yoshifuji, M.; Sasaki, S.; Shiomi, D.; Niitsu, T.; Inamoto, N. *Phosphorus, Sulfur Silicon Relat. Elem.* **1990**, *49-50*, 325. (b) Yoshifuji, M.; Sasaki, S.; Inamoto, N. *J. Chem. Soc., Chem. Commun.* **1989**, 1732. (c) Jutzi, P.; Meyer, U.; Krebs, B.; Dartmann, M. *Angew. Chem. Int. Ed. Engl.* **1986**, *25*, 919. (d) Scholz, M.; Roesky, H. W.; Stalke, D.; Keller, K.; Edelmann, F. T. *J. Organomet. Chem.* **1989**, *366*, 73. (e) Ranaivonjatovo, H.; Escudié, J.; Couret, C.; Satgé, J. *Phosphorus and Sulfur and the Related Elements* **1987**, *31*, 81.
(15) Urnéžius, E.; Protasiewicz, J. D. *Main Group Chemistry* **1996**, *1*, 369.
(16) Sasamori, T.; Takeda, N.; Tokitoh, N. *J. Phys. Org. Chem.* **2003**, *16*, 450.
(17) Sakagami, M.; Sasamori, T.; Sakai, H.; Furukawa, Y.; Tokitoh, N. *Bull. Chem. Soc. Jpn.* **2013**, *86*, 1132.
(18) Bard, A. J.; Cowley, A. H.; Kilduff, J. E.; Leland, J. K.; Norman, N. C.; Pakulski, M.; Heath, G. A. *J. Chem. Soc., Dalton Trans.* **1987**, 249.
(19) Treatment of **9** with ^{n}BuLi in THF at room temperature affords adduct **120**, which exhibits two doublets at δ_P –9 and δ_P 81 ppm ($^1J_{pp}$ = 344 Hz) in its ^{31}P NMR spectrum. The discrepancy of the ^{31}P NMR chemical shifts may be attributed to the measurement of **120** at lower temperature (0 °C). For details, see: Yoshifuji, M.; Shibayama, K.; Inamoto, N. *Chem. Lett.* **1984**, *13*, 115.
(20) Smith, R. C.; Urnezius, E.; Lam, K.; Rheingold, A. L.; Protasiewicz, J. D. *Inorganic Chemistry.* **2002**, *41*, 5296.
(21) (a) Kabuto, C.; Akine, S.; Kwon, E. *J. Cryst. Soc. Jpn.* **2009**, *51*, 218.
(b) Kabuto, C.; Akine, S.; Nemoto, T.; Kwon, E. *J. Cryst. Soc. Jpn.* **2009**, *51*, 218.
(22) (a) Altomare, A.; Burla, M. C.; Camalli, M.; Cascarano, G. L.; Giacovazzo, C.; Guagliardi, A.; Moliterni, A. G. G.; Polidori, G.; Spagna, R. *J. Appl. Crystallogr.* **1999**, *32*, 115. (b) Burla, M. C.; Caliandro, R.; Carrozzini, B.; Cascarano, G. L.; Cuocci, C.; Giacovazzo, C.; Mallamo, M.; Mazzone, A.; Polidori, G. *J. Appl. Crystallogr.* **2015**, *48*, 306.
(23) Sheldrick, G. *Act. Cryst. Sec. C* **2015**, *71*, 3.
(24) Spek, A. *Acta Crystallographica Section D* **2009**, *65*, 148.